

Mitotic progression becomes irreversible in prometaphase and collapses when Wee1 and Cdc25 are inhibited

Tamara A. Potapova^{a,b}, Sushama Sivakumar^c, Jennifer N. Flynn^a, Rong Li^b, and Gary J. Gorbsky^{a,c}

^aCell Cycle and Cancer Biology Research Program, Oklahoma Medical Research Foundation, Oklahoma City, OK 73104; ^bStowers Institute for Medical Research, Kansas City, MO 64110; ^cDepartment of Cell Biology, University of Oklahoma Health Sciences Center, Oklahoma City, OK 73104

ABSTRACT Mitosis requires precise coordination of multiple global reorganizations of the nucleus and cytoplasm. Cyclin-dependent kinase 1 (Cdk1) is the primary upstream kinase that directs mitotic progression by phosphorylation of a large number of substrate proteins. Cdk1 activation reaches the peak level due to positive feedback mechanisms. By inhibiting Cdk chemically, we showed that, in prometaphase, when Cdk1 substrates approach the peak of their phosphorylation, cells become capable of proper M-to-G1 transition. We interfered with the molecular components of the Cdk1-activating feedback system through use of chemical inhibitors of Wee1 and Myt1 kinases and Cdc25 phosphatases. Inhibition of Wee1 and Myt1 at the end of the S phase led to rapid Cdk1 activation and morphologically normal mitotic entry, even in the absence of G2. Dampening Cdc25 phosphatases simultaneously with Wee1 and Myt1 inhibition prevented Cdk1/cyclin B kinase activation and full substrate phosphorylation and induced a mitotic “collapse,” a terminal state characterized by the dephosphorylation of mitotic substrates without cyclin B proteolysis. This was blocked by the PP1/PP2A phosphatase inhibitor, okadaic acid. These findings suggest that the positive feedback in Cdk activation serves to overcome the activity of Cdk-opposing phosphatases and thus sustains forward progression in mitosis.

Monitoring Editor

Mark J. Solomon
Yale University

Received: Jul 15, 2010

Revised: Jan 28, 2011

Accepted: Feb 3, 2011

INTRODUCTION

The eukaryotic cell cycle is driven by the activities of cyclin-dependent kinases (Cdks). Cdks belong to a family of heterodimeric serine/threonine protein kinases, consisting of two subunits: a catalytic subunit and an activating subunit termed a cyclin. In budding and fission yeast, a single Cdk associates with a number of cyclins to drive the entire cell cycle. Metazoans express a number of Cdks. Cdk1, activated by cyclin B, is the primary driver of mitosis, and it phosphorylates a large number of substrates. In budding yeast, ~200 Cdk1 protein substrates have been identified; however, the estimated number could be as high as 500, or roughly 8% of the

entire yeast proteome (Ubersax *et al.*, 2003). Analysis of human proteins associated with the mitotic spindle revealed a total of more than 700 phosphorylated serine and threonine sites in 260 proteins (Nousiainen *et al.*, 2006). Most of these phospho-serines and phospho-threonines were followed by proline residues, suggesting that they are phosphorylated by Cdk1. Another recent large-scale mass spectrometry study evaluated total protein phosphorylation in mitotic HeLa cells and identified phosphorylations on more than 3500 proteins (Dephoure *et al.*, 2008). The majority of these phosphorylation sites fit the Cdk consensus, suggesting that all these proteins may be Cdk1 substrates in human cells. Phosphorylation can affect proteins in a number of ways; it can activate or inhibit them, alter binding to other proteins, or change subcellular localization.

Cyclin B accumulates and binds to Cdk1 during S and G2 phases of the cell cycle. However, the Cdk1/cyclin B complex is inhibited by phosphorylation on inhibitory T14 and Y15 prior to mitotic entry. Two kinases are responsible for the inhibitory phosphorylation: Wee1 and Myt1. Their action is opposed by a group of dual-specificity phosphatases termed Cdc25 phosphatases. In interphase, Wee1 and Myt1 are active, Cdc25 is inactive, and the Cdk activity is low. Wee1, Myt1, and Cdc25 are themselves Cdk1 substrates.

This article was published online ahead of print in MBoC in Press (<http://www.molbiolcell.org/cgi/doi/10.1091/mbc.E10-07-0599>) on February 16, 2011.

Address correspondence to: Tamara A. Potapova (tpo@stowers.org).

Abbreviations used: APC/C, anaphase-promoting complex/cyclosome; Cdk, cyclin-dependent kinase; GFP, green fluorescent protein; FRET, fluorescence resonance energy transfer.

© 2011 Potapova *et al.* This article is distributed by The American Society for Cell Biology under license from the author(s). Two months after publication it is available to the public under an Attribution–Noncommercial–Share Alike 3.0 Unported Creative Commons License (<http://creativecommons.org/licenses/by-nc-sa/3.0>). “ASCB®,” “The American Society for Cell Biology®,” and “Molecular Biology of the Cell®” are registered trademarks of The American Society of Cell Biology.

Active Cdk1 phosphorylates and inhibits Wee1 and Myt1 kinases and phosphorylates and activates the Cdc25 phosphatases. These effects of active Cdk1 on Wee1/Myt1 and on the Cdc25 phosphatases comprise two positive feedback mechanisms, where active Cdk1 inhibits its inhibitors and activates its activator (Supplemental Figure 1). These feedback mechanisms can produce rapid autoamplification of Cdk1 activity (Novak and Tyson, 1993; Tyson and Novak, 2001).

The activity of the Cdk1/cyclin B kinase is high until the mitotic spindle checkpoint is satisfied, when cyclin B is targeted for degradation by an E3 ubiquitin ligase, the anaphase-promoting complex/cyclosome (APC/C) (Glotzer *et al.*, 1991; Clute and Pines, 1999) associated with its activator Cdc20 (Kallio *et al.*, 1998). Importantly, active Cdk1 also activates its own inhibitor, the APC/C, by phosphorylation (Hershko *et al.*, 1994; Lahav-Baratz *et al.*, 1995; Sudakin *et al.*, 1995; King *et al.*, 1996). However, prior to anaphase onset, the degradation of most APC/C-Cdc20 substrates is prevented by the mitotic spindle checkpoint. The spindle checkpoint, which itself requires Cdk activity, prevents initiation of cyclin B proteolysis until all chromosomes achieve stable bipolar attachment to the mitotic spindle (Musacchio and Salmon, 2007). Then the APC/C-Cdc20 inactivates Cdk1 by targeting cyclin B for degradation. In this manner, Cdk1 activates its own inhibitor, the APC/C, establishing a negative feedback loop that turns off Cdk1, allowing the cell to exit mitosis (Supplemental Figure 1).

Turning off Cdk1 allows dephosphorylation of substrates that were phosphorylated in mitosis, and this dephosphorylation underlies mitotic exit. The dephosphorylation of mitotic substrates is carried out by serine/threonine phosphatases, whose identity and regulation are far less explored than that of kinases. In yeast, the primary phosphatase that catalyzes dephosphorylation of Cdk1 substrates during mitotic exit is Cdc14 (Stegmeier and Amon, 2004). In higher eukaryotes, this role appears to be carried out by PP1 and PP2A subfamilies of serine/threonine phosphatases (De Wulf *et al.*, 2009). PP1 and PP2A belong to the PPP (phosphoprotein phosphatase) family (Andreeva and Kutuzov, 2001). Members of PPP family are multimeric enzymes: PP1 holoenzymes consist of catalytic, regulatory, and sometimes inhibitory subunits; and PP2A holoenzymes consist of catalytic, scaffolding, and regulatory subunits. Although there is little diversity among catalytic subunits, the repertoire of regulatory subunits is very broad. Different combinations of catalytic and regulatory subunits generate a large variety of phosphatase holoenzyme complexes. In the past, phosphatases were often perceived as promiscuous, constitutively active enzymes. More recent research indicates that at least some phosphatases are very specific and their activity is tightly regulated, spatially and temporally (Virshup and Shenolikar, 2009). Currently, much remains to be learned about specificities and regulation of phosphatase holoenzymes in mitosis, but it is becoming clear that phosphatases participate in opposing kinases at all stages of mitotic progression, from mitotic entry to mitotic exit (Bollen *et al.*, 2009).

Here we show that cells become capable of “forward” (M-to-G1) mitotic progression after the prophase stage, in prometaphase and metaphase. In the course of transition from prophase to prometaphase, phosphorylation of Cdk1 substrates increases sharply, reflecting the spike of Cdk1 activity in the cell. Hence, cells become committed to forward mitotic progression around the peak of Cdk1 substrate phosphorylation. Interfering with the positive feedback mechanisms that mediate rapid and complete activation of Cdk1 causes cells to fail mitosis, a state we term “mitotic collapse,” in which mitotic substrates became dephosphorylated without cyclin

B breakdown. This substrate dephosphorylation depended on okadaic acid-sensitive phosphatases, suggesting that the biological purpose of feedback-mediated Cdk activation may be to overcome the activity of Cdk-opposing phosphatases and to sustain mitosis.

RESULTS

Cells commit to forward M-to-G1 transition at prometaphase

APC/C-dependent proteolysis of mitotic regulators is the key element of the “forward” (M-to-G1) mitotic transition (Sullivan and Morgan, 2007). To determine when during mitosis inactivation of Cdk1 results in a “forward” transition, cells were treated with the chemical Cdk inhibitor Flavopiridol at different stages of mitosis. Flavopiridol inactivates Cdk1 and triggers rapid mitotic exit at any point in mitosis. Importantly, Cdk inhibition allows APC/C-Cdc20 to target its substrates for degradation before the spindle checkpoint is satisfied. We have previously shown that Flavopiridol triggers degradation of the Cdk1 activator cyclin B in cells arrested in mitosis with nocodazole (Potapova *et al.*, 2006, 2009). Depletion of Cdc20 by small interfering RNA (siRNA) confirmed that normal degradation of cyclin B and securin induced by chemical Cdk1 inhibitor required normal levels of APC/C-Cdc20 but not APC/C-Cdh1 (Figure 1A).

We defined the point of commitment to “forward” mitotic transition as the stage when APC/C-Cdc20 becomes proficient to process mitotic substrates in response to Cdk inhibition. In other words, Cdk inhibitor was used as a tool to determine when during mitosis APC/C-Cdc20 becomes capable of targeting its substrates for destruction. We tested the proficiency of the APC/C-Cdc20 to target endogenous cyclin B by observing the ability of cells to re-enter mitosis after washout of Cdk1 inhibitor Flavopiridol. Flavopiridol is a reversible Cdk inhibitor. When it is washed out after induction of mitotic exit, cells can re-enter mitosis if cyclin B is preserved (Potapova *et al.*, 2006). However, turning off Cdk activates Wee1 and Myt1 kinases that inhibit Cdk by phosphorylation. They can lock Cdk in an inactive state even if cyclin B is preserved (Kapuy *et al.*, 2009; Potapova *et al.*, 2009). To circumvent this feedback-mediated inhibition, we treated the cells with PD0166285, a chemical inhibitor of Wee1/Myt1 kinases (Wang *et al.*, 2001; Li *et al.*, 2002; Hashimoto *et al.*, 2006). Under these conditions, the ability of cells to re-enter mitosis depended solely on the preservation of cyclin B. Therefore assaying reversibility gave us a tool to test APC/C-Cdc20 activation during mitotic exit induced by the Cdk inhibitor.

For these experiments, we imaged live *Xenopus* S3 cells expressing alpha-tubulin tagged with green fluorescent protein (GFP). Cells were treated with Flavopiridol and PD0166285 at specific stages of mitosis from prophase to metaphase for 1 h, and then Flavopiridol was washed out. The results, summarized in Figure 1B, indicated that cells exited mitosis permanently only when Cdk was inhibited after nuclear envelope breakdown.

If cells were treated with Cdk inhibitor in prophase, mitotic progression stopped, chromosomes decondensed, and cells became indistinguishable from ordinary interphase cells. When Cdk inhibitor was washed out after 1 h, these cells re-entered mitosis and were capable of normal mitotic progression (Figure 1C and Supplemental Video 1). This result indicated that the cyclin B in these cells was preserved. Thus, during prophase, cells respond to Cdk1 inhibitor by retreating to a G2-like state. This finding may be reminiscent of the observations on the “antephase checkpoint,” the ability of some cell lines to reversibly undo mitotic entry when exposed to various stress factors in prophase (Matsusaka and Pines, 2004; Mikhailov *et al.*, 2005).

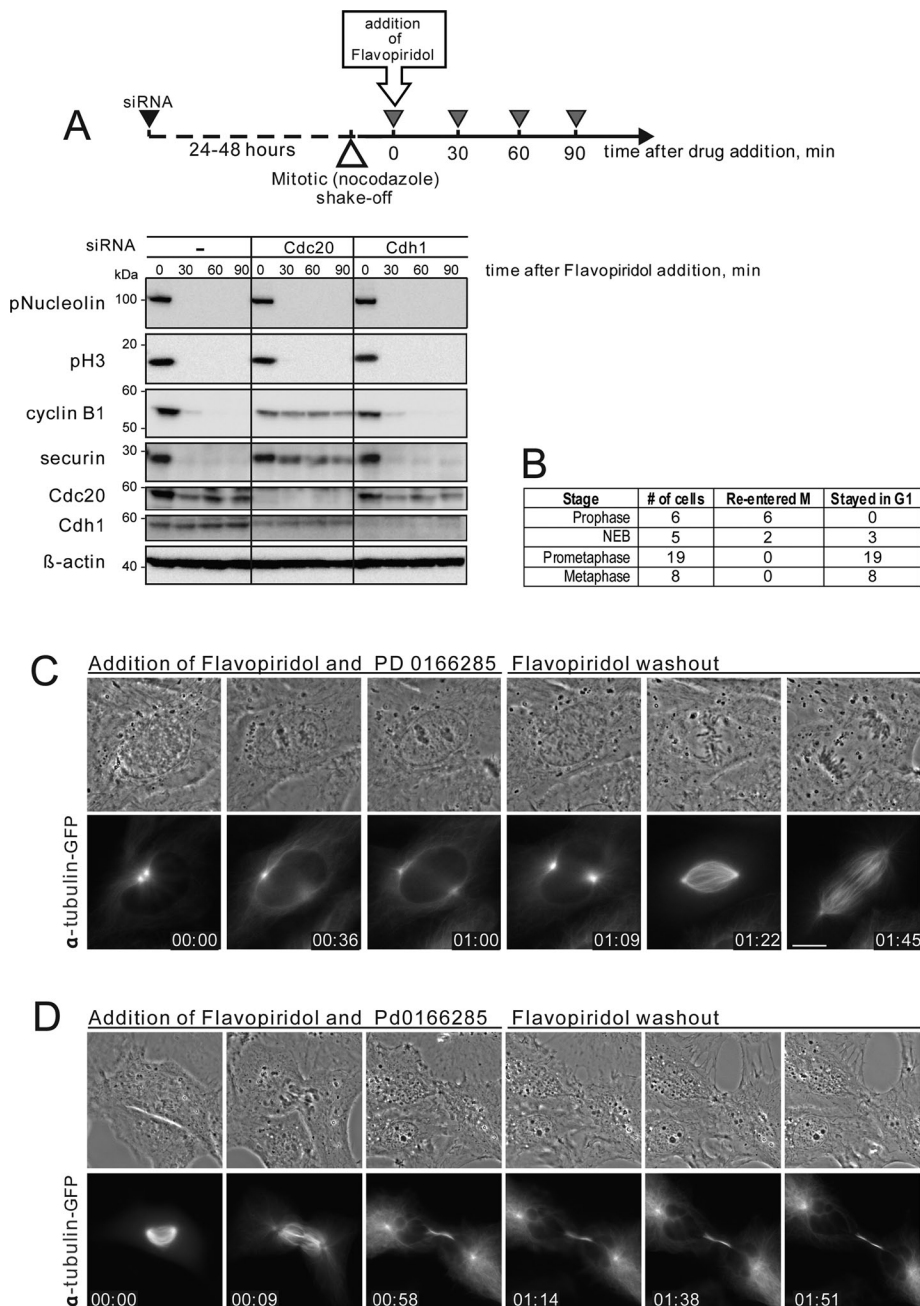


FIGURE 1: Cells commit to forward mitotic progression in prometaphase. (A) Chemical Cdk inhibition in mitosis induces cyclin B1 and securin degradation that requires APC/C-Cdc20. HeLa cells were transfected with 50 nM Cdc20 siRNA for 24 h or with 50 nM Cdh1 siRNA for 48 h. Mitotic cells were collected in nocodazole, treated with 10 μ M Flavopiridol for 30, 60, and 90 min, then lysed and processed for Western blotting. Depletion of Cdc20, but not Cdh1, inhibits degradation of cyclin B and securin. (B) Summary of the live imaging data from *Xenopus* S3 cells treated with Cdk inhibitor, Flavopiridol, and Wee1/Myt1 inhibitor, PD 0166285 at different stages of the mitotic progression. Flavopiridol was washed out 1 h after addition. (C) A prophase *Xenopus* S3 cell expressing alpha tubulin-GFP was treated with Cdk inhibitor, Flavopiridol, and Wee1/Myt1 inhibitor, PD 0166285. After treatment with Cdk inhibitor, mitotic progression stopped, the chromosomes decondensed, and the cell returned to an interphase morphology. Flavopiridol was washed out at 1 h, and the cell re-entered mitosis, indicating that Cdk1-activating cyclins were preserved. The cell then progressed normally through mitosis. (D) An early prometaphase *Xenopus* S3 cell expressing alpha tubulin-GFP was treated with Flavopiridol and PD 0166285. After treatment at time 0, the cell underwent cytokinesis without chromosome segregation, the chromosomes decondensed, the nuclear envelope reformed, and an interphase array of microtubules appeared. Flavopiridol was washed out at 1 h. However, the cell did not re-enter mitosis, indicating that it had advanced to a G1-like state. The complete time-lapse sequences for (A) and (B) are shown in Supplemental Videos 1 and 2. Bar, 10 μ m.

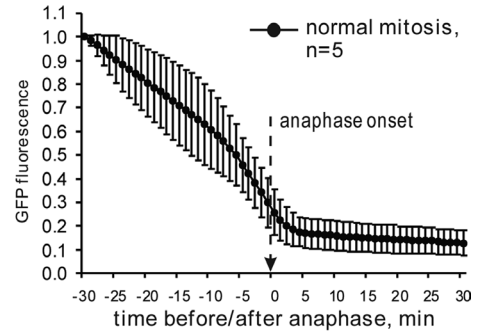
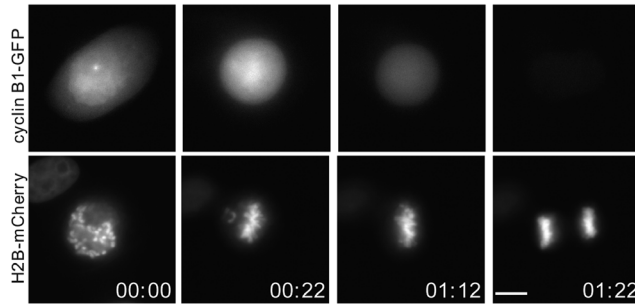
In contrast, when cells were treated with the Cdk inhibitor at any point in prometaphase or metaphase, they underwent cytokinesis, decondensed chromosomes, reformed nuclear envelopes, and established interphase arrays of microtubules. Washing out the inhibitor 1 h after its addition did not result in mitotic re-entry (Figure 1D and Supplemental Video 2). Lack of mitotic entry was consistent with the interpretation that most cyclin B was degraded in these cells. Thus, during prometaphase or metaphase, cells respond to Cdk1 inhibitor by advancing to a G1-like state. Overall, Cdk inhibition in prophase results in "backtracking" from M back to G2, whereas Cdk inhibition after prophase results in forward mitotic progression.

The experiments mentioned above had the advantage of using endogenous cyclin B to regulate Cdk1 activity and cell cycle responses but did not allow us to assess the dynamics of its degradation directly. To quantify the degradation of cyclin B in living cells at different stages of mitosis, we transfected HeLa cells with plasmids encoding human cyclin B fused to fluorescent proteins. Wild-type human cyclin B1 fused with GFP was transiently transfected in HeLa cells stably expressing histone H2B tagged with mCherry. Levels of cyclin B were monitored by time-lapse fluorescence microscopy.

Cyclin B is cytoplasmic during interphase and rapidly translocates into the nucleus in prophase (Pines and Hunter, 1991; Clute and Pines, 1999; Hagting *et al.*, 1999). After nuclear envelope breakdown, cyclin B disperses throughout the cytoplasm with a propensity to accumulate on the mitotic spindle, chromosomes, and unattached kinetochores (for details, see Bentley *et al.*, 2007). In normal cell cycle progression, proteolysis of exogenously expressed, fluorescently tagged cyclin B begins at metaphase, with most cyclin B being degraded before the onset of anaphase (Clute and Pines, 1999). Consistent with previous reports, in our experiments the bulk of cyclin B-GFP disappears shortly before anaphase onset (Figure 2A and Supplemental Video 3).

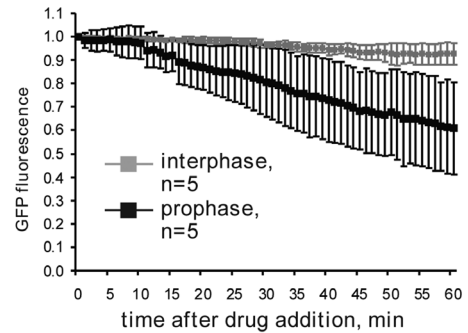
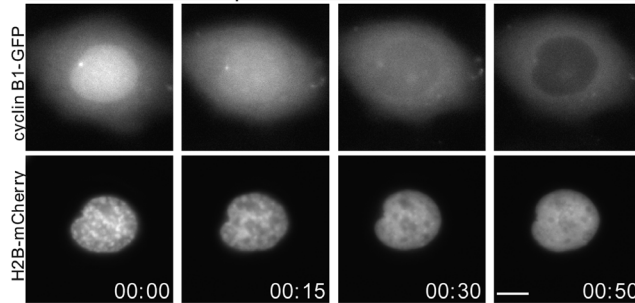
In cells treated with the Cdk inhibitor in prophase, immediately after the translocation of cyclin B-GFP in the nucleus, cyclin B breakdown was slow and variable. On Flavopiridol addition, the fluorescence intensity of cyclin B1-GFP decreased very slowly, dropping on average 30–35% after 1 h (Figure 2B and Supplemental Video 4). This result supported the conclusion from mitotic re-entry experiments in *Xenopus* S3 cells that the APC/C-Cdc20 is incompletely

A - normal mitosis



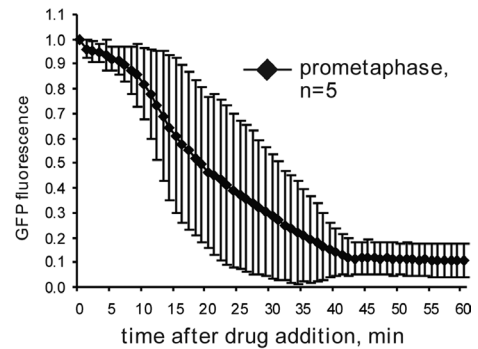
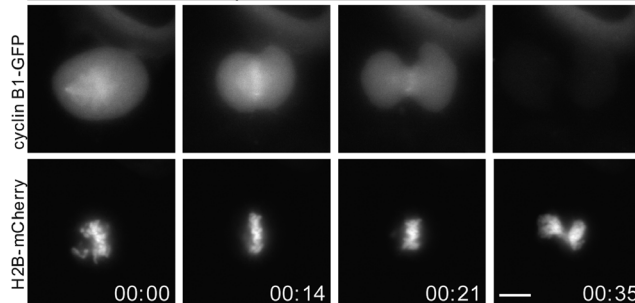
B - prophase cell

Addition of Flavopiridol



C - prometaphase cell

Addition of Flavopiridol



D - metaphase cell

Addition of Flavopiridol

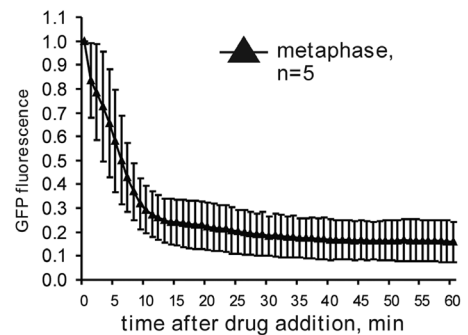
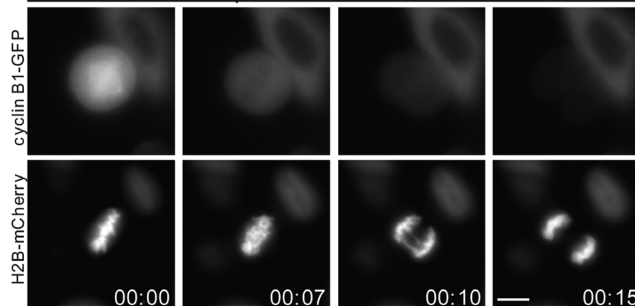


FIGURE 2: Cdk1 inhibition after prophase induces cyclin B degradation. (A) HeLa cells expressing wild-type cyclin B1-GFP and histone H2B-mCherry through normal mitosis. At left is an example of live cell imaging of a HeLa cell transiting mitosis. At right is plotted normalized cyclin B1-GFP intensity starting 30 min before anaphase onset for 5 cells. (B) Prophase, (C) prometaphase, and (D) metaphase HeLa cells expressing cyclin B1-GFP were treated with Flavopiridol at time 0. Flavopiridol induced chromosome decondensation and degradation of cyclin B. At left are examples of time-lapse imaging. On the right, normalized fluorescence intensity of the GFP is plotted starting from the time of Flavopiridol addition for five cells from each stage of mitosis. The rate of Flavopiridol-induced cyclin B degradation increases with the stage of mitosis. Complete time-lapse sequences for (A–D) are shown in Supplemental Videos 3–6. Bar, 10 μ m.

competent to target cyclin B for degradation during prophase. Also, when mitotic progression stopped and the chromosomes decondensed after Flavopiridol addition, cyclin B translocated out of the nucleus in most cases. Our observation that cyclin B-GFP is exported from the nucleus in response to Cdk inhibition in prophase agrees with the report by Gavet and Pines (2010a).

In sharp contrast, Cdk inhibition in prometaphase and metaphase cells resulted in proteolysis of most cyclin B (Figure 2, C and D, and Supplemental Videos 5 and 6). However, the degradation kinetics varied depending on the stage of mitotic progression. Metaphase cells degraded most of their cyclin B within 10 min after Cdk inhibition, and most metaphase cells segregated chromatids. Prometaphase cells degraded cyclin B more slowly, with most of their cyclin B gone in 30 min. Prometaphase cells invariably failed to segregate chromatids, resulting in chromosomes being trapped within the cleavage furrow—the “cut” phenotype. Similar results were observed in cells transfected with cyclin B1 tagged with DsRed (data not shown). These results are consistent with the interpretation that APC/C-Cdc20 becomes increasingly more competent for ubiquitylation of cyclin B with progression through mitosis after prophase.

Together, these data suggest that Cdk inhibition after prophase results in forward cell cycle progression. However, prometaphase cells exhibited slower cyclin B breakdown and an inability to segregate chromosomes. This may be attributed to a failure to fully activate APC/C-Cdc20. The APC/C is phosphorylated in mitosis on multiple sites primarily by Cdk1, but also by Plk1 and possibly other kinases (Steen *et al.*, 2008). The exact functional significance of each phosphorylation is not known, but replacing some of them with residues that cannot be phosphorylated hinders the catalytic activity of the complex (Vodermaier and Peters, 2004). The functional studies indicate that the phosphorylation of APC/C subunits promotes binding of Cdc20 (Shteinberg *et al.*, 1999; Kramer *et al.*, 2000; Rudner and Murray, 2000). Hence, reduction of the APC/C phosphorylation in mitosis may hinder its ability to process substrates whose degradation depends on APC/C-Cdc20. The indirect evidence that this indeed may be the case comes from studies using the Cdk1AF mutant, which lacks inhibitory phosphorylation sites. Cdk1AF short-circuits the Wee1 and Cdc25 feedback loops, causing Cdk1 activity to oscillate rapidly but with lower amplitude. Importantly, this also leads to reduced APC/C activity (Pomerening *et al.*, 2005). All this, together with our results, led us to hypothesize that the amplitude of Cdk1 activity is the key determinant for the “forward” directionality of mitotic progression. We next investigated the dynamics of Cdk activation during mitotic entry by analyzing the phosphorylation of its substrates.

Cdk1 activity increases sharply during prophase and prometaphase

It is well established that the activity of Cdk1/cyclin B complex is low in interphase and high in mitosis, but the direct measurement of Cdk1/cyclin B activation in intact individual cells has been a challenge. Work in the embryonic *Xenopus* egg extract system showed that Cdk1 activation is rapid and complete in response to the threshold concentration of its activator, cyclin B (Pomerening *et al.*, 2003; Sha *et al.*, 2003). However, mitotic entry is a continuous process, and we next explored when and how fast Cdk1 is activated in cells entering mitosis. We measured the Cdk1 activity in individual cells by quantifying immunofluorescence labeling of HeLa cells with three antibodies, MPM2, pS-Cdk, and phospho-nucleolin, that bind endogenous mitotic phosphoepitopes. The fluorescence intensity of antibody labeling was measured at different stages of mitotic pro-

gression, from prophase to metaphase. To precisely define mitotic stage, cells were costained for DNA and Lamin B.

MPM2 antibody recognizes a large number of proteins that are phosphorylated in mitosis, predominantly by Cdk1 (Davis *et al.*, 1983). MPM2 antibody stained brightly the nucleus and spindle poles in prophase. After nuclear envelope breakdown, the labeling dispersed throughout cytoplasm with some concentration at the mitotic spindle. Quantitative analysis of the integrated intensity showed that the MPM2 signal sharply increased in prophase but also continued to rise during prometaphase (Figure 3A). Representative images are shown in Supplemental Figure 2A.

Phospho-(Ser) CDKs substrate antibody (pS-Cdk) is a commercially available antibody (Cell Signaling, Beverly, MA) that detects phosphorylated serine in a Cdk substrate motif (K/R)(pS)PX(K/R). pS-Cdk antibody labeled prophase nuclei similarly to MPM2, and then appeared dispersed throughout the cytoplasm in prometaphase (Supplemental Figure 2B). Analysis of the pS-Cdk labeling also indicated a steep rise in intensity during prophase. The fluorescence intensity continued to increase in prometaphase, when the signal spread throughout the cytoplasm (Figure 3B).

Phospho-nucleolin antibody recognizes the ribonuclear protein nucleolin at a site phosphorylated specifically by Cdk1 (Dranovsky *et al.*, 2001). This protein localizes to the nucleoli of interphase cells and is dispersed throughout cytoplasm in mitosis, with some concentration of protein enveloping condensed chromosomes. Phospho-nucleolin antibody exclusively labels mitotic cells and colocalizes with the total nucleolin labeling (Supplemental Figure 3). Phospho-nucleolin labeling serves as a reliable *in vivo* readout for Cdk1/Cyclin B activity (Potapova *et al.*, 2006, 2009). Phosphorylated nucleolin appeared at detectable levels in the nucleus in early prophase, when chromosomes begin to condense. The nucleolus disassembles during prophase, when many of its structural components become phosphorylated (reviewed in Boisvert *et al.*, 2007). Phosphorylation of nucleolin increased sharply and rapidly, beginning from the onset of nucleoli disassembly in prophase and continuing even after nucleoli were completely disassembled (for representative images, see Supplemental Figure 2C). Similar to the other markers, phospho-nucleolin labeling increased sharply throughout prophase and prometaphase (Figure 3C). Thus, using these markers of endogenous Cdk1 phosphorylation targets, Cdk1 activity rises sharply in prophase and continues to rise after nuclear envelope breakdown.

From these experiments, we concluded that the bulk of Cdk activation occurs in pro- and prometaphase. This conclusion is generally consistent with the previous immunofluorescence studies (Lindqvist *et al.*, 2007) and recent FRET analyses (Gavet and Pines, 2010a, 2010b). As shown in Figures 1 and 2, cells become irreversibly committed to mitosis in prometaphase. Therefore commitment to mitosis occurs when the large part of Cdk substrates is phosphorylated (Figure 3B).

Mitosis fails in the absence of positive feedback during Cdk activation

Next, we investigated the relative importance of the timing of Cdk1/cyclin B activation versus the feedback-mediated dynamics of its activation. For this, we evaluated the mitotic progression in cells entering mitosis prematurely and in cells where the positive feedback of Cdk1 was reduced.

The Wee1/Myt1 inhibitor PD0166285 abrogates the G2 DNA damage checkpoint and causes mitotic entry (Wang *et al.*, 2001; Hashimoto *et al.*, 2006). Applying this drug to the asynchronous cultures of various cell lines led to the emergence of a large number of mitotic cells. Presumably these were from the G2 subpopulation.

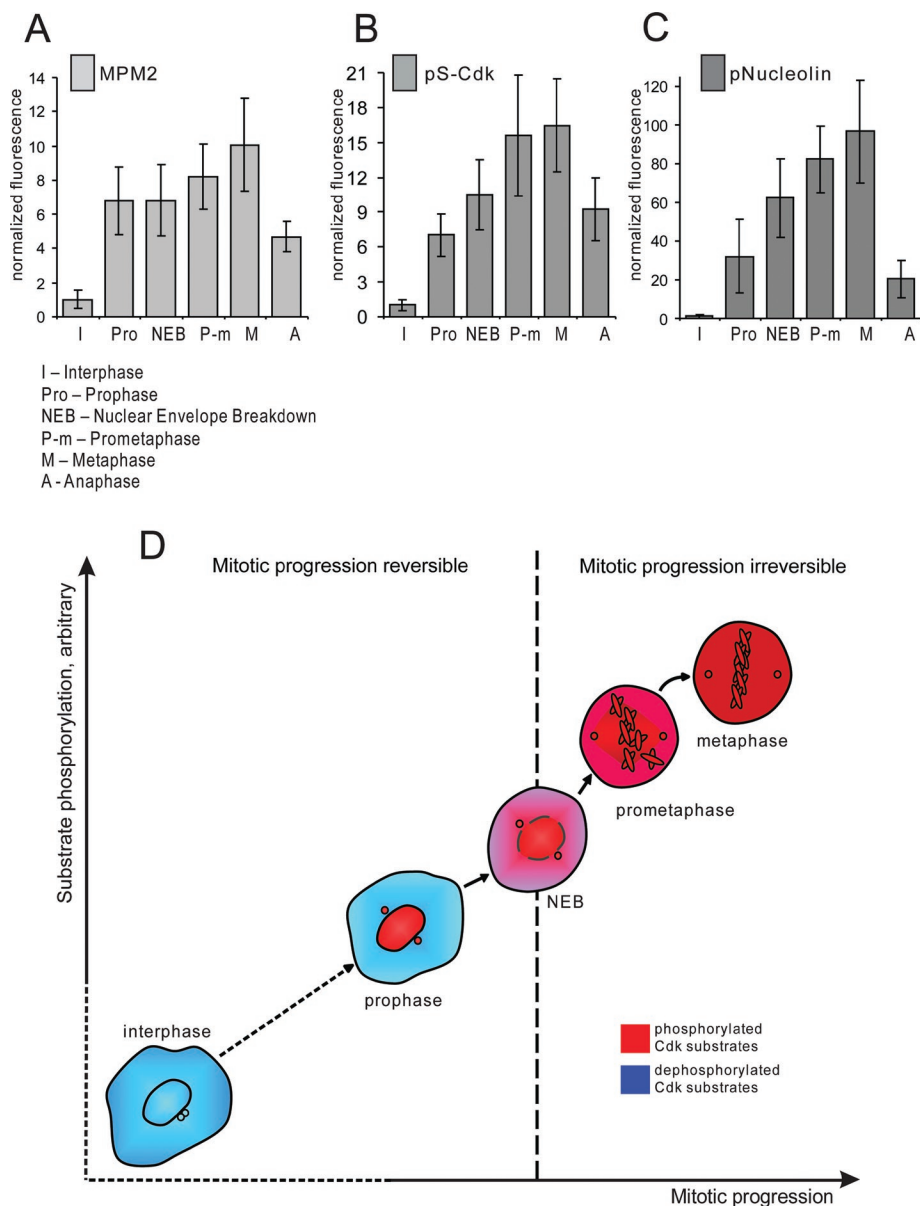


FIGURE 3: Cdk1 phosphoepitopes rise rapidly during early mitosis. HeLa cells synchronized by double thymidine block were fixed 9 h after the release from the second thymidine block and immunolabeled with following antibodies: MPM2 (A), pS-Cdk (B), and pNucleolin (C). The fluorescence intensities were plotted according to mitotic stage. To assess the stage of mitosis precisely, cells were costained with antibody against Lamin B and with DNA dye. Integrated fluorescence intensity of a cell was measured at the brightest plane of a z series taken at 1- μ m intervals. Each bar on the graphs represents an average of 15–30 cells for each stage. Error bars denote standard deviation. Representative images of each stage are shown in Supplemental Figure 2. (D) Diagram depicting relationship between Cdk substrate phosphorylation and irreversible mitotic entry. Cells become committed to forward mitotic progression in prometaphase, when Cdk substrates become phosphorylated.

We used the Wee1/Myt1 inhibitor to stimulate premature mitotic entry at the end of the S phase. For this, HeLa cells were synchronized by double thymidine block, released, and treated with PD0166285 at the end of S phase (see the diagram in Figure 4). After release from the second thymidine block, HeLa cells are in S-phase for about 6 h and the subsequent G2 takes 2–6 h. Mitotic entry typically begins at ~8 h after release with about half of the cells being in mitosis by 10 h. Addition of the Wee1/Myt1 inhibitor at the end of the S-phase (6 h after second thymidine release) completely

overrode the G2 delay and triggered strikingly rapid and massive mitotic entry (Figure 4A and Supplemental Video 7). Most cells were able to build normal mitotic spindles and align chromosomes at the metaphase plate (Figure 4, A and C). Anaphase was not visibly perturbed, and chromosomes segregated after complete alignment at the metaphase plate. This suggested that the mitotic spindle checkpoint and the APC/C were functioning in cells that entered mitosis without G2.

Subsequent experiments addressed the ability of cells to progress through mitosis when the positive dephosphorylation of Cdk1 on inhibitory T14 and Y15 by Cdc25 was compromised. Chemical inhibition of Cdc25 should slow down activation of Cdk1. To accomplish this, we treated HeLa cells synchronized at the end of S-phase with the Wee1/Myt1 inhibitor PD0166285 and the Cdc25 inhibitor NSC663284 (Pu *et al.*, 2002). The simultaneous inhibition of Wee1/Myt1 kinases and Cdc25 phosphatases blocks both phosphorylation and dephosphorylation of Cdk1 inhibitory residues. Surprisingly, many of the synchronized cells treated with combination of Wee1/Myt1 and Cdc25 inhibitors entered prophase at nearly the same time as cells treated with Wee1/Myt1 inhibitor alone (Figure 4B). However, cells treated with Wee1/Myt1 and Cdc25 inhibitors remained in prophase with condensed chromosomes two to three times longer than untreated cells or cells treated with Wee1/Myt1 inhibitor alone. Rounding up of the cells, characteristic for mitotic entry, was also slower. Most significantly, subsequent mitotic progression was entirely perturbed. After prophase, cells treated with Wee1/Myt1 and Cdc25 inhibitors failed to achieve a metaphase chromosome alignment and did not segregate chromatids or undergo anaphase. Approximately 1–2 h later, the chromosomes partially decondensed but stayed in the middle of the cell. There was no concurrent blebbing of the cell membrane or shrinkage of the cytoplasm characteristic of cell death. Most cells did not flatten down and remained round (Figure 4B and Supplemental Video 8). Cells remained in this state for several hours before showing signs of apoptosis such as membrane blebbing. Based on this morphology and biochemical analyses reported below we termed this phenotype “mitotic collapse,” meaning an aborted mitotic entry and failure to progress through mitosis.

In asynchronously growing cell cultures, simultaneous inhibition of Wee1/Myt1 and Cdc25 also induced mitotic collapse in cells that entered mitosis 20–30 min after the addition of both inhibitors. In HeLa cells expressing fluorescent mCherry–histone H2B and tubulin-GFP, prolonged prophase was followed by extended prometaphase-like state. Then the mitotic spindle partially disassembled

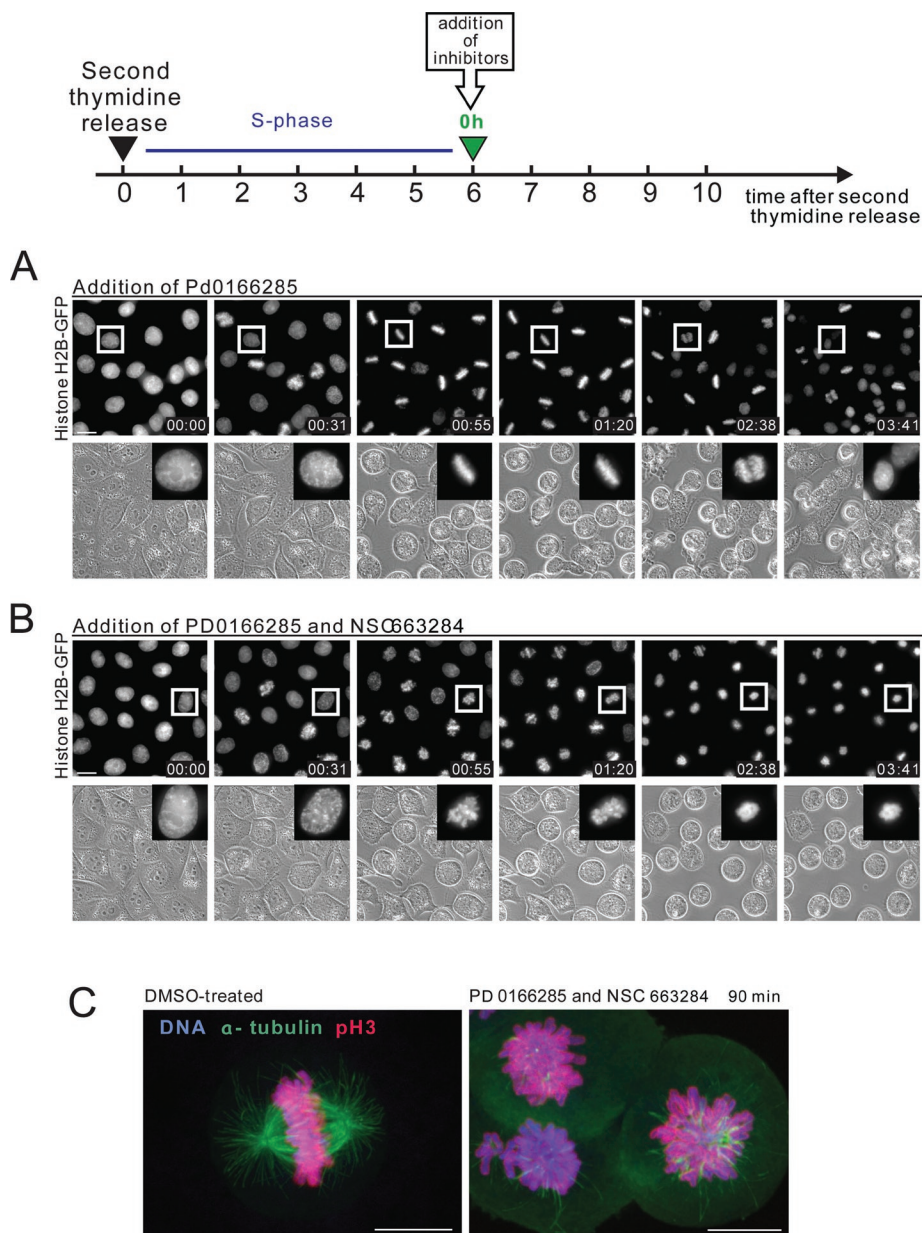


FIGURE 4: Mitotic progression in cells synchronized at S/G2 and treated with Wee1/Myt1 and Cdc25 inhibitors. (A, B) HeLa cells stably expressing fluorescent histone H2B fused to GFP were synchronized by the double thymidine block at the S/G2 border and treated with the Wee1/Myt1 inhibitor, PD0166285, alone (A) or in combination with Cdc25 inhibitor, NSC663284 (B). While the Wee1/Myt1 inhibitor alone rapidly triggers mitosis in the majority of cells, the combination of the Wee1/Myt1 and Cdc25 inhibitors results in slow mitotic entry followed by mitotic collapse. The complete time-lapse sequence is shown in Supplemental Videos 7 and 8. Bar, 10 μ m. (C) Synchronized HeLa cells were treated with the Wee1/Myt1 inhibitor, PD0166285, alone or in combination with Cdc25 inhibitor, NSC663284, for 90 min. Cells were then fixed and processed by immunofluorescence for alpha-tubulin and phosphorylated-histone H3 on S10 (mitotic marker). Labeling shows disorganized mitotic spindle, and in some cells, reduced mitotic marker.

and chromatin packed around the spindle poles (Supplemental Figure 5A and Video 9). To rule out the possibility that this phenomenon may be specific for HeLa cells, similar results were obtained with RPE-1 hTERT cells stably expressing histone H2B-GFP (Supplemental Figure 4B and Video 10). Treatment with inhibitors did not affect the morphology or viability of cells that remained in interphase during the experiment.

nation of Wee1/Myt1 and Cdc25 inhibitors (180 min after drug addition), the fluorescence intensities of these markers plunged compared with cells that remained arrested in mitosis in Wee1/Myt1 inhibitor alone.

This result was perplexing because the active spindle checkpoint triggered by depolymerized microtubules should have prevented the activation of APC/C-Cdc20 and mitotic exit. Moreover, the

To examine the mitotic collapse phenotype in more detail, synchronized HeLa cells were treated with a combination of Wee1/Myt1 and Cdc25 inhibitors for 90 min and immunolabeled for alpha-tubulin and phospho-S10 histone H3, a commonly used early mitotic marker, phosphorylated by the mitotic kinase aurora B (Wei et al., 1999). The labeling confirmed that the mitotic collapse phenotype was characterized by a disorganized mitotic spindle and unaligned chromosomes in most of the cells (Figure 4C). Interestingly, the phospho-histone H3 labeling was notably reduced in some of these collapsing cells, suggesting that H3 may be undergoing dephosphorylation.

To further characterize the effects of Wee1/Myt1 and Cdc25 inhibition, cells were synchronized and treated with inhibitors as in previous experiments, except that nocodazole was added to the medium to block cells from exiting mitosis. Samples were collected from 6 to 10 h after second thymidine release and analyzed by flow cytometry (Figure 5A) and Western blotting (Figure 5B).

For flow cytometry analysis, cells were fixed and stained with mitotic marker antibody against phospho-histone H3 conjugated to Alexa Fluor 647 fluorophore. In untreated cells, mitotic entry began at ~8 h after the second thymidine release with more than half the cells entering mitosis by 10 h (Figure 5A, blue line). Addition of the Wee1/Myt1 inhibitor at the end of the S-phase triggered a rapid increase in mitotic index that remained high throughout the experiment (Figure 5A, green line). Cdc25 inhibitor by itself prevented mitotic entry (Figure 5A, brown line). When Wee1/Myt1 and the Cdc25 were simultaneously inhibited, phospho-histone H3 increased during the first 2 hours after the treatment, albeit more slowly than in cells treated with Wee1/Myt1 inhibitor alone. However, after 2 hours, the mitotic index dropped (Figure 5A, orange line). The loss of phospho-histone H3 labeling indicated that cells cotreated with Wee1/Myt1 and Cdc25 inhibitors were unable to stay in mitosis in nocodazole. The eventual dephosphorylations of Cdk1 substrates nucleolin, mitotic phosphopeptides MPM2, and pS-Cdk were further confirmed by immunofluorescence experiments (Supplemental Figure 5). In cells that underwent mitotic collapse after treatment with combination of Wee1/Myt1 and Cdc25 inhibitors (180 min after drug addition), the fluorescence intensities of these markers plunged compared with cells that remained arrested in mitosis in Wee1/Myt1 inhibitor alone.

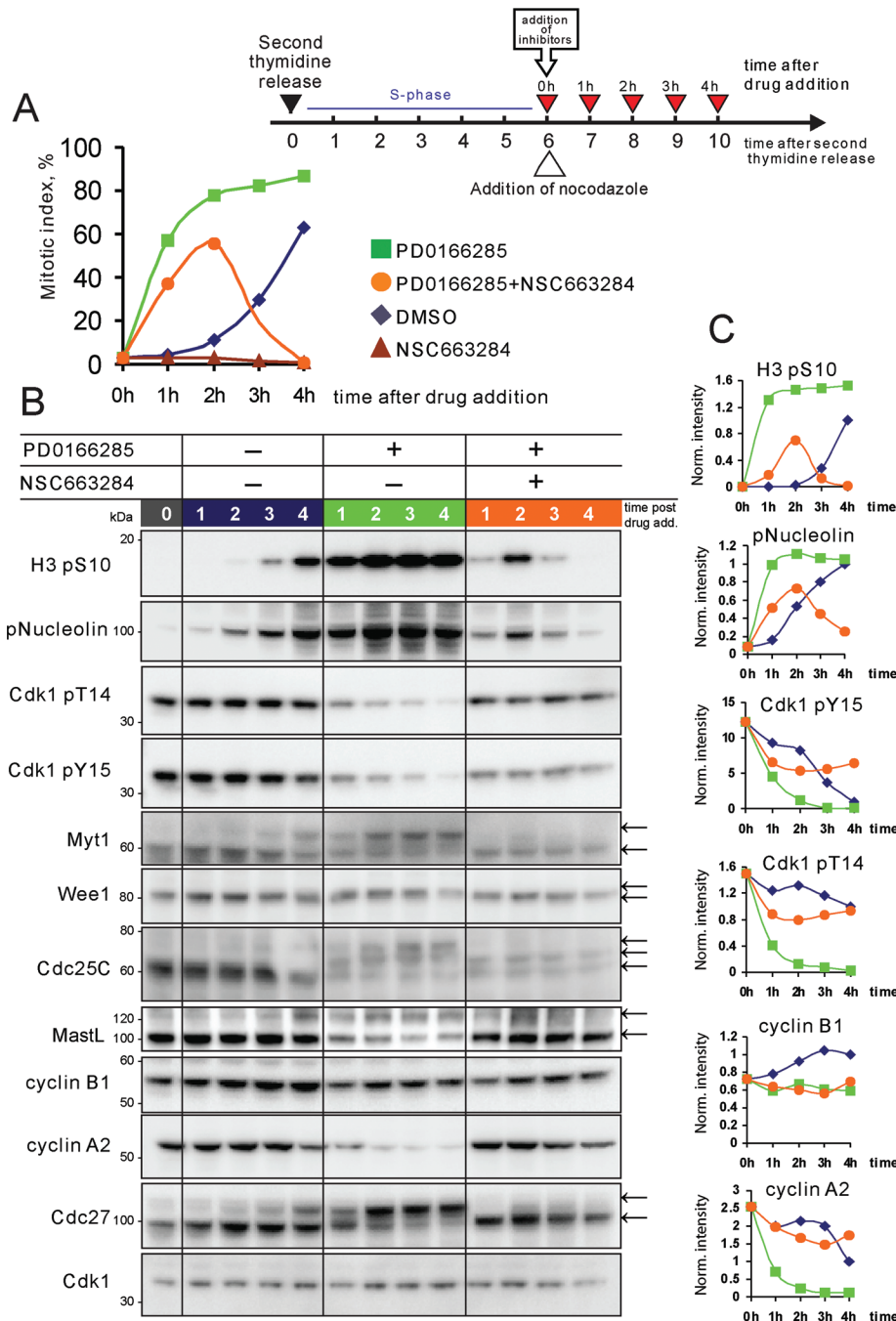


FIGURE 5: Inhibition of Wee1/Myt1 and Cdc25 in synchronized cells causes mitotic collapse. (A) HeLa cells were synchronized at the S/G2 border after double thymidine block and then treated with the Wee1/Myt1 inhibitor, PD0166285, Cdc25 inhibitor, NSC663284, and the combination of the two drugs. Nocodazole was added to the medium to prevent mitotic exit. Cells were then collected at indicated time points, fixed and stained with antibody to phosphohistone H3 (mitotic marker) conjugated with Alexa Fluor 647, and processed by flow cytometry. In cells treated with vehicle only (DMSO, blue line), the mitotic index progressively increased, with more than half the cells being in mitosis by the end of the experiment. Cdc25 inhibitor, NSC663284, blocked mitotic entry during the first hour after its addition. In cells treated with both PD0166285 and NSC663284 (orange line), the mitotic index first increased then fell. (B) HeLa cells were treated as in (A), lysed and analyzed by SDS-PAGE. In cells not treated with inhibitors (blue lanes), phosphorylations on histone H3 and nucleolin appeared by 8 h after second thymidine release and increased for the duration of the experiment. Phosphorylation of Cdk1 on inhibitory T14 and Y15 decreased over time, indicating the activation of the Cdk1/cyclin B complex. As cells were entering mitosis, a portion of Wee1, Myt1, Cdc25C, Cdc27, and MastL acquired an electrophoretic mobility shift. Cyclin B1 levels were increasing, and cyclin A2 levels dropped

mitotic collapse phenotype observed by live imaging was distinct from ordinary mitotic exit. This prompted us to explore the mitotic collapse phenotype further by conducting a biochemical analysis of cell cycle proteins in these cells. Consistent with the flow cytometry data, Western blotting analysis showed that, in cells cotreated with Wee1/Myt1 and Cdc25 inhibitors, phosphorylation of histone H3 was transient, whereas in cells not treated with Cdc25 inhibitor, it remained high. Nucleolin, a direct Cdk1 substrate, became dephosphorylated similarly to histone H3 (Figure 5B).

When cells treated with Wee1/Myt1 inhibitor but not treated with the Cdc25 inhibitor were entering mitosis, the inhibitory residues T14 and Y15 on Cdk1 became dephosphorylated, consistent with the activation of Cdk1. Wee1 and Myt1 acquired electrophoretic mobility shifts characteristic of phosphorylated and inactive forms of these kinases (McGowan and Russell, 1995; Watanabe *et al.*, 1995; Booher *et al.*, 1997; Kim *et al.*, 2005). One of the Cdk-activating phosphatases, Cdc25C, also shifted up, characteristic of its phosphorylated and active form (Izumi and Maller, 1993; Hoffmann *et al.*, 1994). The APC/C subunit Cdc27 (APC3) also displayed a shift corresponding to its mitotically phosphorylated form (Peters *et al.*, 1996). Cyclin B1 levels were increasing slightly, consistent with its accumulation in G2/M (Cogswell *et al.*, 1995; Hwang *et al.*, 1995; Piaggio *et al.*, 1995). Cyclin A2

slightly as cells accumulated in mitosis. Inhibition of Wee1 and Myt1 kinases with PD0166285 (green lanes) resulted in rapid phosphorylation of Nucleolin and histone H3 that peaked 2 h after the drug addition and remained steadily high for the duration of the experiment. Cdk1 was rapidly dephosphorylated on inhibitory T14 and Y15. Wee1, Myt1, Cdc25, and Cdc27 rapidly shifted up. By 1 h after drug addition, Cyclin A2 was largely degraded and cyclin B1 was stable. Inhibition of Wee1 and Myt1 together with Cdc25 by addition of both PD0166285 and NSC 663284 (orange lanes) triggered the a weak phosphorylation on Nucleolin and histone H3 that peaked at 1–2 h and disappeared at 3–4 h after addition of the two drugs. Reduced mitotic phosphorylation shifts of Wee1, Myt1, Cdc25, and Cdc27 indicated that these proteins were not fully phosphorylated. Note that cyclin B and most of the cyclin A were not degraded in these cells. Panels on the right show quantifications of indicated Western blots. All values were adjusted for loading and normalized to the 4-h time point of DMSO-treated cells.

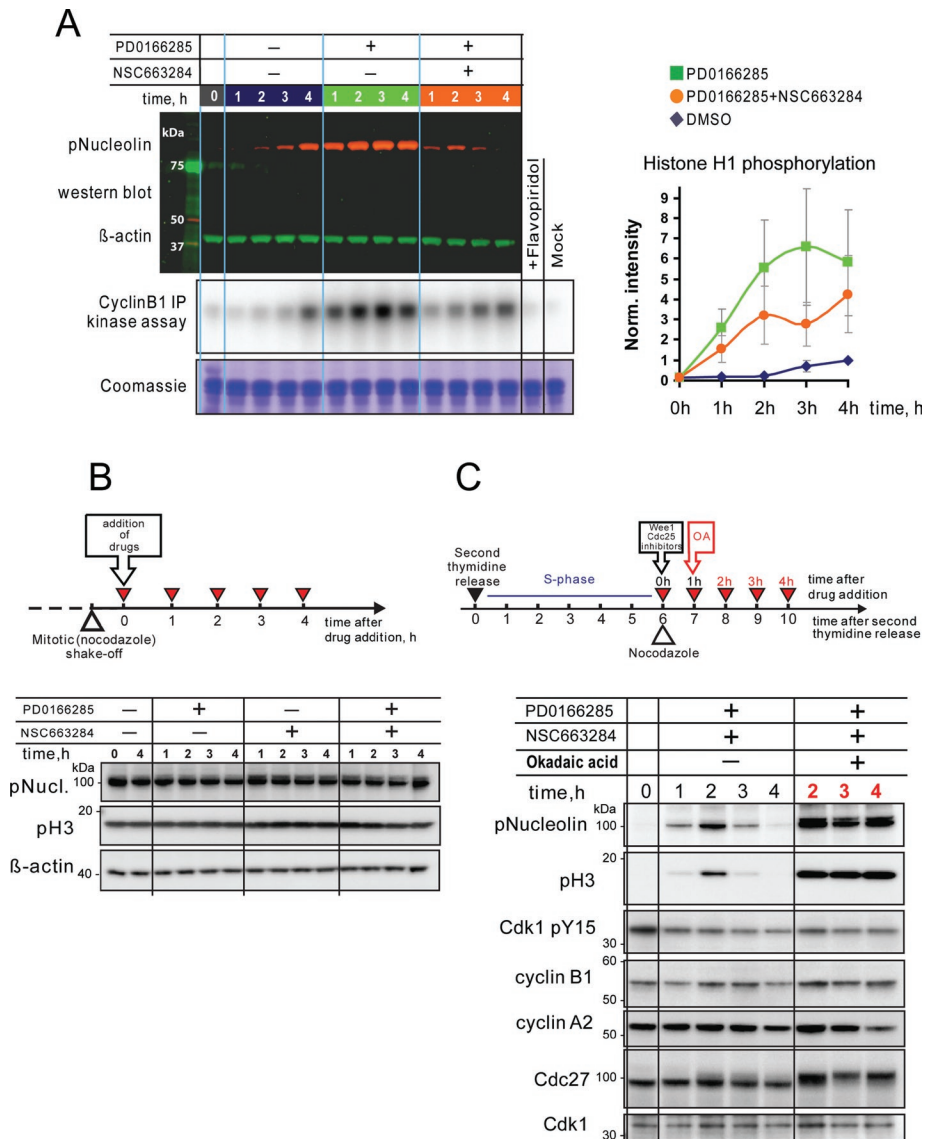


FIGURE 6: Dephosphorylation of mitotic substrates in “collapsed” cells is a result of incomplete inhibition of Cdk-opposing phosphatases. (A) Cdk1/cyclin B1 activity does not drop in mitotic collapse cells. HeLa cells were synchronized at the S/G2 border and treated with the Wee1/Myt1 inhibitor, PD0166285, Cdc25 inhibitor, NSC663284, and the combination of the two in the presence of nocodazole. Cells were then collected at indicated time points and lysed. An aliquot of the lysate was analyzed by Western blotting for Nucleolin phosphorylation. β -Actin served as a loading control. Cyclin B1/Cdk1 complex was immunoprecipitated from the rest of the lysate and subjected to an in vitro kinase assay using histone H1 as a substrate. The kinase reaction mixture was resolved by SDS-PAGE, and the gel was exposed to phosphor-screen, which was then scanned with phosphor-imager. For a control, samples derived from the 4-h time point of DMSO-treated cells were treated with Cdk inhibitor (lane labeled “+Flavopiridol”), or processed omitting cyclin B1 antibody from immunoprecipitation (lane labeled “mock”). The gel was subsequently stained with Coomassie blue for loading. Panel on the right shows quantifications of histone H1 phosphorylation normalized to the 4 h time point of DMSO-treated cells. An average of three independent assays is shown. Error bars denote SD. (B) Simultaneous inhibition of Wee1/Myt1 and Cdc25 in cells already in mitosis does not cause mitotic substrate dephosphorylation. Mitotic HeLa cells were collected in nocodazole and then treated with Wee1/Myt1 and Cdc25 inhibitors for the indicated time, lysed, and analyzed by Western blotting. Mitotic substrates nucleolin and histone H3 remained phosphorylated throughout the experiment. (C) The phosphatase inhibitor, okadaic acid, prevents dephosphorylation of mitotic substrates in cells treated with a combination of Wee1/Myt1 and Cdc25 inhibitors. HeLa cells were synchronized at the S/G2 border after double thymidine block and treated with the Wee1/Myt1 inhibitor, PD0166285, and Cdc25 inhibitor, NSC663284, for the indicated time in the presence or absence of okadaic acid. Addition of the okadaic acid resulted in robust and sustained phosphorylation of mitotic substrates.

levels dropped as cells accumulated in mitosis, because cyclin A is targeted for degradation by the APC/C despite the active mitotic checkpoint (den Elzen and Pines, 2001; Geley *et al.*, 2001). Because mitotic entry was more rapid and synchronous, these changes were more pronounced in cells treated with Wee1/Myt1 inhibitor (Figure 5B, green lanes) than in cells not treated with inhibitor (Figure 5B, blue lanes).

When Wee1 and Myt1 were inhibited together with Cdc25 (Figure 5B, orange lanes), inhibitory residues T14 and Y15 of Cdk1 remained phosphorylated. Some reduction in phosphorylation of T14 and Y15 may be attributed to incomplete inhibition of Cdc25C by NSC 663284, since this inhibitor is most potent for Cdc25A (Pu *et al.*, 2002). The weak phosphorylation of mitotic markers and slight phosphorylation shifts of Wee1, Myt1, Cdc25, and Cdc27 at 1–2 h after drug addition in these cells may have been indicative of low Cdk1 activity, high Cdk-opposing phosphatase(s) activity, or both. One of the inhibitors of Cdk-opposing phosphatases is Greatwall kinase (human MastL). MastL is a Cdk1/cyclin B substrate, and it undergoes a mitotic phosphorylation shift that may correspond to its activation (Burgess *et al.*, 2010; Voets and Wolthuis 2010). A portion of MastL protein showed a phosphorylation shift in cells that entered mitosis but not in cells undergoing mitotic collapse. This may hint that, in the absence of feedback-mediated activation of Cdk1, those phosphatases that are inhibited through MastL remain active.

The most striking result of this experiment was that, whereas mitotic substrates became dephosphorylated 3–4 h after the drug addition, cyclins A and B were not degraded. Therefore the dephosphorylation of mitotic substrates in this case was not caused by inactivation of Cdk through proteolysis of cyclins, as it is in normal mitotic exit. It also was not due to the increase of inhibitory phosphorylation on Cdk1, because the Wee1 and Myt1 are inhibited by PD0166285. In fact, in vitro kinase assays of immunopurified Cdk1/cyclin B1 complex did not show a decrease in kinase activity as its substrate, nucleolin, became dephosphorylated (Figure 6A). Importantly, in cells that were already in mitosis at the time of drug addition, simultaneous inhibition of both Wee1 and Cdc25 did not cause mitotic substrate dephosphorylation (Figure 6B). Thus, the mitotic collapse phenotype may be interpreted as the inability to sustain mitotic phosphorylation in the absence of the feedback-amplified activation of Cdk1 during mitotic entry.

The positive feedback loop in Cdk1 activation is required to overcome Cdk-opposing phosphatases

The mitotic collapse phenotype, observed in cells treated with both Wee1/Myt1 and Cdc25 inhibitors, was accompanied by the dephosphorylation of mitotic substrates but not cyclin proteolysis or Cdk1 inactivation by phosphorylation. A phosphatase or phosphatases that oppose the action of mitotic kinases were able to dephosphorylate their substrates when the positive feedback on Cdk1 was abrogated. This suggests that there may have been a balance of phosphorylation and dephosphorylation reactions that eventually shifted toward dephosphorylation when the feedback-mediated Cdk activation was prevented. Therefore the activation of Cdk1 by positive feedback during mitotic entry may be required to overcome the activity of Cdk-opposing phosphatases.

To test whether phosphatase activity played a direct role in the mitotic collapse phenotype, we applied the phosphatase inhibitor, okadaic acid, at 1 μ M 1 h after the treatment of synchronized cells with Wee1/Myt1 and Cdc25 inhibitors, before mitotic substrates became dephosphorylated. The addition of okadaic acid prevented dephosphorylation of nucleolin and histone H3, consistent with the involvement of PP1- or PP2A-like phosphatases to the mitotic collapse phenotype (Figure 6C). Importantly, okadaic acid also increased the phosphorylation of nucleolin, histone H3, and Cdc27 when the levels of phosphorylation of inhibitory Y15 residue of Cdk1 remained steady, providing evidence for the counterbalance of the kinase and phosphatase activities in mitosis. Unfortunately, because okadaic acid by itself induces strong perturbations in cytoplasmic and nuclear morphology unrelated to the cell cycle, we were not able to assess whether phosphatase inhibition could fully rescue the mitotic collapse phenotype by morphological criteria.

These results indicated that blocking the activity of phosphatases allowed mitotic substrates to remain phosphorylated when positive feedback of Cdk1 activation was suppressed. Failure to amplify Cdk1 activity through rapid dephosphorylation of inhibitory residues leads to the mitotic collapse, which we argue is a direct consequence of the inability to overcome Cdk-opposing phosphatases. Together, these results highlight the importance of the feedback-mediated Cdk1 activation for shifting the kinase–phosphatase balance toward mitotic phosphorylation.

DISCUSSION

Mitotic progression requires a wave of Cdk1 activity that phosphorylates a large number of substrates. However, the details of how this wave of phosphorylation coordinates the precisely ordered physiological processes of mitosis are incompletely understood. A particularly important issue that awaits explanation is the relationship between mitotic kinases and their antagonistic phosphatases. Here, we show that cells become capable of the “forward” M-to-G1 cell cycle transition only after Cdk1 is fully activated. Under normal circumstances, positive feedback-mediated Cdk1 activation may function to overcome the activity of Cdk1-opposing phosphatases. This mode of Cdk activation appears to be essential for maintaining the mitotic state and for the proper ordering of mitotic events.

By chemically inhibiting Cdk1 at different stages of mitosis from prophase to metaphase, we demonstrated that Cdk1 inhibition results in complete cyclin B breakdown and irreversible cell division (“forward” mitotic transition) only if the Cdk inhibitor was applied after prophase. Application of Cdk inhibitor in prophase caused return to interphase without substantial cyclin B breakdown, and cells could re-enter mitosis when the Cdk inhibitor was removed. Thus, Cdk inhibition in prophase induces cells to retreat back to G2. Estimation of the Cdk1 activity at different stages of mitotic progression

by immunofluorescence analysis of the phosphorylation of three mitotic substrates revealed that the rapid rise of Cdk1-mediated phosphorylation occurs primarily during the short transition from prophase to prometaphase. This is generally consistent with previous immunofluorescence measurements by Lindqvist *et al.* (2007), where Cdk activation was assessed by measuring the dephosphorylation of the inhibitory Y15 on Cdk1 and phosphorylation of the Cdk1 substrate APC/C subunit Cdc27 (Lindqvist *et al.*, 2007). More recently, Gavet and Pines were able to measure the activity of Cdk1/cyclin B complex in individual cells directly, by using a FRET biosensor designed specifically for Cdk1/cyclin B1 kinase (Gavet and Pines 2010a, b). This elegant molecular tool used a short fragment of human cyclin B1 harboring an autophosphorylation site. This biosensor exhibited a steep increase in FRET signal during prophase and early prometaphase. Overall, this trend was similar to the one observed in our immunofluorescence experiments. Taken together, these data point toward the conclusion that the rapid increase of Cdk1 activity in prometaphase determines the moment when cells become committed to “forward” mitotic progression.

The primary indicator for “forward” mitotic progression in our studies was proteolysis of cyclin B, which depends on the activation of APC/C-Cdc20. APC/C-Cdc20 is itself a Cdk substrate that is heavily phosphorylated in mitosis (Kraft *et al.*, 2003; Herzog *et al.*, 2005; Steen *et al.*, 2008). Even though we did not assess APC/C phosphorylation directly due to the lack of suitable phosphoepitope antibodies, we anticipate the kinetics of APC/C phosphorylation to be similar to that of the other mitotic substrates we did assess. Lindqvist *et al.* (2007) performed quantitative analysis of mitotic phosphorylation of specific Cdk1 target residues on one of the subunits of the APC/C–Cdc27/APC3–T446 and S426. Their study showed that the bulk of these residues became phosphorylated during prophase and prometaphase (Lindqvist *et al.*, 2007). In our study, live imaging analysis of fluorescent cyclin B breakdown induced by Cdk inhibition showed that, functionally, APC/C-Cdc20 becomes progressively more efficient at targeting cyclin B for degradation with advancing stages of mitosis. Therefore activation of Cdk1 is likely to be a determining factor for the ability of the APC/C-Cdc20 to process mitotic substrates.

Our immunofluorescence analysis showed that there is considerable variability in final (metaphase) levels of Cdk1 activity from cell to cell. However, this variability did not seem to impact mitotic progression. The final level of Cdk1/cyclin B activity in the cell is likely determined by the amount of cyclin B because Cdk1 was reported to be in vast excess over cyclins in cells (Arooz *et al.*, 2000). Several cyclin B knockdown studies reported a variety of relatively minor mitotic perturbation in different cell lines, suggesting that overall mitotic progression has room to be remarkably tolerant to reduction of cyclin B levels by siRNA or shRNA (Yuan *et al.*, 2004, 2006; Bellanger *et al.*, 2007; Gong *et al.*, 2007; Androic *et al.*, 2008; Chen *et al.*, 2008). Although the efficiency of knockdown may partially explain the weak phenotype, this observation is also consistent with the idea that the total level of Cdk1/cyclin B activity is less important than the positive feedback-mediated rapidity of Cdk activation. For instance, overexpression of the Cdk1-AF mutant, which lacks inhibitory phosphorylation sites, causes a profound effect on cell cycle progression, manifested by premature chromatin condensation, aberrant mitosis, and abbreviated cell cycles (Jin *et al.*, 1996; Pomeroy *et al.*, 2008; Gavet and Pines, 2010b). This phenotype was somewhat distinct from the mitotic collapse phenotype, particularly in the aspect of persistent oscillations between mitotic and interphase state that were not observed in our experiments. However, in the above studies, Cdk1-AF mutant was overexpressed

above the endogenous wild-type Cdk1. Therefore a portion of Cdk1/cyclin B complex in these studies may have been assembled with endogenous, wild-type Cdk1 that retained the ability to be regulated by phosphorylation.

In this study, we used fast-acting chemical inhibitors to analyze the importance of the switch-like activation of endogenous Cdk1 for the proper order of mitotic progression. Inhibition of the Wee1 and Myt1 kinases in cells induced a relatively normal mitosis in cells synchronized at the end of S phase, without requiring a G2 stage. Ordinarily, during G2, cells grow and accumulate various proteins, including mitotic cyclins. In cells pushed into mitosis by the Wee1/Myt1 inhibitor, cyclin B1 did not accumulate to the level characteristic of cells that entered mitosis without the inhibitor. Surprisingly, the amount of cyclin B present by the end of the S phase in synchronized cells was sufficient for entry into mitosis. Because inhibition of Wee1 and Myt1 kinases resulted in rapid dephosphorylation of Cdk1 on inhibitory T14 and Y15, Cdk1 activation in these cells was still rapid, even though their cyclin B levels were lower than in cells that entered mitosis spontaneously. Nevertheless, these cells were able to progress through mitosis, supporting the idea that, for the proper order of mitotic events, the final Cdk1 activity levels may be less critical than the feedback-mediated dynamics of its activation.

Simultaneous inhibition of Wee1/Myt1 kinases and Cdc25 phosphatases prevented both phosphorylation and dampened dephosphorylation of Cdk1 on inhibitory T14 and Y15. Unexpectedly, this led to a sluggish mitotic entry followed by dephosphorylation of mitotic substrates without cyclin B breakdown—a phenotype that we termed “mitotic collapse.” The failure to degrade cyclin B likely reflects insufficient activation of APC/C-Cdc20 by low levels of Cdk1 activity, similar to the situation in prophase cells. The substrate dephosphorylation was prevented by 1 μ M okadaic acid, indicating that the Cdk1 was actively antagonized by phosphatase(s).

The possibility that the combination of Wee1 and Cdc25 inhibitors could have some off-target effect that can influence phenotypic changes observed in cells undergoing mitotic collapse cannot be completely excluded. This caveat is intrinsic to any chemical inhibitor studies. However, it is highly unlikely that these inhibitors can trigger the nonspecific phosphatase activation, because phosphorylation of nucleolin and histone H3 was not lost in cells that were already in mitosis at the time of drug addition (Figure 6B).

Historically, mitosis research has highlighted the mitotic kinases as key regulators of cell division, whereas phosphatases have received much less attention. However, it is becoming clear that the normal progression of mitosis is not only a consequence of the change in activity of mitotic kinases, primarily Cdk1, but requires balanced actions of counteracting phosphatases (Trinkle-Mulcahy and Lamond, 2006).

In budding yeast, the primary phosphatase opposing Cdk1 is Cdc14 (Visintin *et al.*, 1998; Jaspersen *et al.*, 1999; reviewed in Stegmeier and Amon, 2004; Bosl and Li, 2005; Amon, 2008). However, in metazoans, neither of the two Cdc14 homologues, Cdc14A or Cdc14B, has been shown to counteract Cdk1 kinase during mitotic exit (Vazquez-Novelle *et al.*, 2005; Berdougou *et al.*, 2008). Instead, in higher eukaryotes, the PP1 and PP2A families of protein phosphatases, enzymes that can be inhibited by okadaic acid, appear to play more important roles in mitotic entry and exit. In *Xenopus* egg extracts, depletion studies have implicated both PP1 and PP2A in the dephosphorylation of Cdk1 substrates (Mochida *et al.*, 2009; Wu *et al.*, 2009). Interestingly, both PP1 and PP2A phosphatases appear to be inhibited by high Cdk1 activity, constituting another feedback mechanism where the Cdk1 kinase inactivates its antagonists, shifting the balance toward mitotic phosphorylation (Figure 7A)

PP1 is phosphorylated by Cdk1 on the inhibitory T320 residue (Dohadwala *et al.*, 1994; Kwon *et al.*, 1997; Wu *et al.*, 2009). When Cdk1 is inactivated during mitotic exit, PP1 activates itself by dephosphorylating this T320 residue and another residue, T35 (likely a MAP kinase site), responsible for the binding of the inhibitory protein I-1 (Wu *et al.*, 2009). Another small protein inhibitor of PP1 is the inhibitory protein 2 (I-2), which is also heavily phosphorylated in mitosis (Li *et al.*, 2007) and may be a Cdk1 substrate. Therefore the activation of Cdk1 may switch PP1 off, and inactivation of Cdk1 may switch PP1 on. Further experimental and modeling studies are needed to evaluate the dynamics and robustness of this switch.

A similar mechanism of Cdk-dependent inhibition may exist for PP2A. The activity of PP2A-B55 delta is low when Cdk1 is fully active in mitosis (Mochida and Hunt, 2007). Unlike PP1, PP2A has not yet been shown to be inhibited by Cdk1 phosphorylation directly. However, a kinase called Greatwall (human MastL) has been shown to inhibit anti-mitotic phosphatases in the *Xenopus* egg extract system (Castilho *et al.*, 2009; Vigneron *et al.*, 2009). Greatwall kinase is a Cdk1/cyclin B substrate. Active Cdk1/cyclin B complex phosphorylates and activates Greatwall, which then inhibits PP2A and perhaps other phosphatases, constituting another feedback loop that promotes mitotic phosphorylation (Figure 7A).

Because the substrate of the human MastL kinase is not yet identified, we were not able to assay its activity directly. By Western blotting, we observed a phosphorylation shift during mitotic entry that was absent in mitotic collapse, suggesting that MastL may be inactive in collapsed cells (Figure 5B). This may partially explain the elevated phosphatase activity in these cells. MastL knockdown was shown to cause defects in chromosome alignment and segregation and also incomplete cyclin B breakdown upon mitotic exit (Burgess *et al.*, 2010; Voets and Wolthuis, 2010). However, strong MastL knockdown as well as the Greatwall depletion in *Xenopus* egg extracts were reported to block entry in mitosis. We attempted to override this block in MastL siRNA-treated HeLa cells synchronized at the S/G2 border by treating them with the Wee1/Myt1 inhibitor PD0166285. The mitotic entry in this case was comparable in both MastL siRNA and negative control siRNA-treated cells. The phenotype of MastL knockdown cells that entered mitosis in Wee1 inhibitor was generally similar to what has been reported previously (Supplemental Figure 6 and Video 11), although there was an increased incidence of mitotic cell death. We did not observe defects reminiscent of mitotic collapse, which suggests that MastL may be responsible for inhibition of some, but not all Cdk-opposing phosphatases involved in generating mitotic collapse phenotype. Alternatively, the depletion of MastL by siRNA may have been insufficient to fully release phosphatase activities.

The phosphatase(s) responsible for the mitotic collapse phenotype in our studies likely belonged to the PP2A family because the dephosphorylation of mitotic substrates was prevented by 1 μ M okadaic acid. At this concentration, PP1 is only partially inhibited (Bialojan and Takai, 1988). Okadaic acid not only prevented the dephosphorylation of Cdk1 substrates but also markedly increased their phosphorylation (Figure 6C). Without okadaic acid, mitotic phosphatases eventually overcame Cdk activity when it was not fueled by positive feedback, resulting in mitotic collapse. One possible mechanism that may aid somatic cells in countering phosphatase activity during mitotic entry is spatial concentration of Cdk1 activity within the nucleus in early mitosis. Cdk1/cyclin B complex translocates into the nucleus in prophase and then disperses throughout the cytoplasm after nuclear envelope breakdown (Pines and Hunter, 1991; Hagting *et al.*, 1998). It was recently confirmed that translocation of Cdk1/cyclin B complex into the nucleus coincides with its

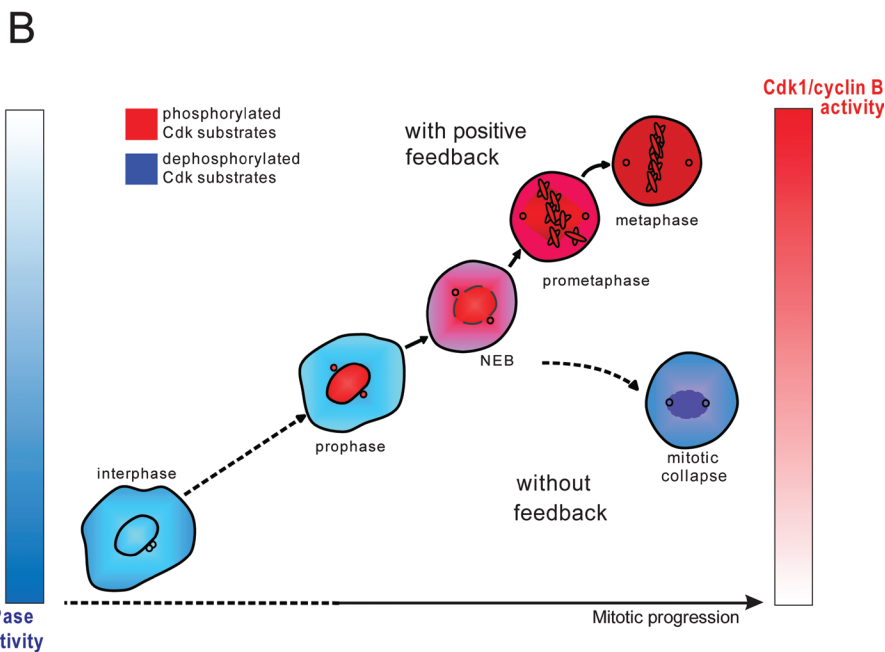
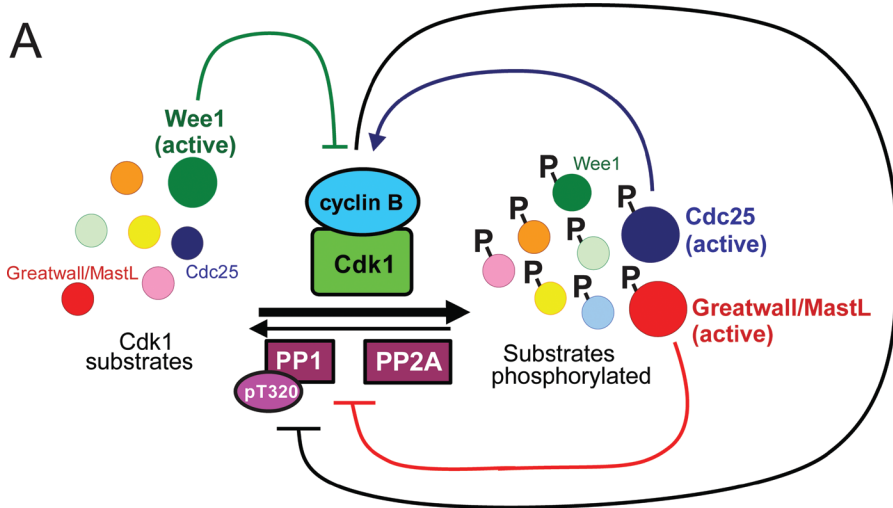


FIGURE 7: (A) Cdk substrate phosphorylation regulatory network. The phosphorylation of mitotic substrates (enzymes and structural proteins) by Cdk1/cyclin B complex underlies mitotic entry. Cdk1/cyclin B is antagonized by phosphatases PP1 and PP2A that dephosphorylate mitotic substrates. Wee1 kinase and Cdc25 phosphatases regulate Cdk1 activity: Wee1 inhibits Cdk1 (green inhibitory line) and Cdc25 activates it (blue arrow). Wee1 and Cdc25 are themselves Cdk substrates. Cdk1 phosphorylates and inhibits Wee1, preventing Wee1 from inactivating Cdk1. Also, Cdk1 phosphorylates and activates its activator Cdc25. Active Cdk also inhibits antagonists PP1 and PP2A by at least two known mechanisms. First, Cdk1 can inhibit PP1 directly by phosphorylating T320 residue on a catalytic subunit of the phosphatase (black inhibitory line). Second, Cdk1 phosphorylates and activates the Greatwall/MastL kinase, which inhibits PP2A and possibly PP1 by yet unidentified mechanisms (red inhibitory line). Therefore as Cdk activation is fueled by positive feedback, it also promotes the inactivation of its antagonists, ensuring the stability of substrate phosphorylation. (B) Failure to activate Cdk rapidly results in mitotic collapse after nuclear envelope breakdown. The feedback-mediated activation of the Cdk1/Cyclin B complex may be required to prevent the dilution of the kinase activity throughout the cytoplasm when the nuclear envelope becomes permeable. Cdk1 activity appears to spike around the time of the nuclear envelope disassembly, when the activated Cdk/cyclin B complex spreads through the cytoplasm. In the absence of the positive feedback, active Cdk1 would be diluted in the cytoplasm when the nuclear envelope becomes permeable. In the absence of positive feedback mechanisms, the concentration of the active kinase per unit of cytosol may fall below the level that is needed to efficiently counteract Cdk-opposing phosphatases, which leads to the mitotic collapse.

activation (Gavet and Pines, 2010a). Consistent with this, our immunolabeling experiments show that the Cdk activity is concentrated in the nucleus in prophase, and after nuclear envelope breakdown, the cytoplasm fills with phosphorylated Cdk1 substrates (Supplemental Figure 2, A–C). Overall, it appears that Cdk1 activity spikes around the time of the nuclear envelope disassembly, when the activated Cdk/cyclin B complex spreads through the cytoplasm. Therefore it is possible that in the absence of the positive feedback, active Cdk1 became too dilute in the cytoplasm when the nuclear envelope disassembled or became permeable enough to permit the diffusion of Cdk1/cyclin complexes out of the nucleus (Figure 7B). Under these circumstances, the concentration of the active kinase per unit of cytosol may have fallen below the level that is needed to efficiently counteract Cdk-opposing phosphatases and maintain mitosis.

The mitotic collapse phenotype that we observed was accompanied by substrate dephosphorylation, but morphologically it was far from normal mitotic exit. Mitotic exit, like mitotic entry, is a well-ordered sequence of events: chromatid segregation is followed by cytokinesis, nuclear envelope reassembly, cytoskeletal rearrangements, etc. Whether this orderly progression requires a particular sequence of dephosphorylation reactions is not known. However, our results suggest that the proper interplay of kinase and phosphatase activities, where feedback-mediated activation of Cdk first overcomes the activity of phosphatases then is rapidly turned off, is essential for the normal mitotic entry and exit.

MATERIALS AND METHODS

Cell culture, plasmid, and siRNA transfection

Xenopus S3 cells were grown at 23°C in 70% L-15 medium supplemented with 15% fetal bovine serum (FBS). HeLa and RPE1 cells (ATCC, Manassas, VA) were grown in DMEM with 10% FBS in 5% CO₂ at 37°C. HeLa cells were transiently transfected using Fugene 6 or Fugene HD (Roche) according to the manufacturer's directions. Plasmid encoding the wild-type human cyclin B1-GFP was a generous gift from Randall King. Live imaging experiments were conducted 24–48 h following the transfection of cyclin B. siRNA targeting Cdc20 and Cdh1 were obtained from Dharmacon/Thermo Scientific (Lafayette, CO; ON-Target plus SMART pool #L-003225-00-0005 for Cdc20, #L-015377-00-0005 for Cdh1, and #L-004020-00-0005 for MASTL). HeLa cells were transfected with the siRNAs

using Lipofectamine RNAi (Invitrogen, Carlsbad, CA) according to the manufacturer's directions.

Chemical inhibitors

The Cdk inhibitor, Flavopiridol (Enzo Life Sciences, Plymouth Meeting, PA) was used at 10 μ M. The proteasome inhibitor MG132 (Calbiochem, San Diego, CA) was used at 25 μ M. The Wee1/Myt1 inhibitor PDO166285 (Pfizer, New York, NY) was used at 0.5 μ M. The Cdc25 inhibitor NSC663284 (Sigma, St. Louis, MO) was used at 25 μ M. The other Cdc25 inhibitor, NSC95397 (Enzo Life Sciences) was used at 10–20 μ M. Okadaic acid (LLC Labs or Alexis Biochemicals, San Diego, CA) was used at 1 μ M. Nocodazole (Sigma) was used at 300 ng/ml.

Drug treatments and Western blotting

For siRNA experiments, mitotic HeLa cells were collected by shake-off 24–48 h after siRNA transfection followed by a 3- to 4-h nocodazole block. The mitotic cells were split into a number of experimental groups and treated with Flavopiridol for indicated periods of time. Cells were then pelleted by centrifugation and lysed in NuPAGE protein sample buffer (Invitrogen) containing 50 mM dithiothreitol (DTT).

For synchronization experiments, HeLa cells were grown in 35-mm plates, synchronized by double thymidine block, and then treated as detailed in figure legends. Each plate represented an experimental sample. Samples were collected by trypsinization and lysed in NuPAGE buffer with 50 mM DTT.

Protein samples were separated by SDS-PAGE in 4–12% Bis-Tris gels (Invitrogen), transferred to PVDF (Millipore, Billerica, MA), and blocked in 5% bovine serum albumin (BSA). Primary antibody against phospho-Nucleolin (pNucleolin) was a generous gift from Peter Davies; cyclin A2 AT-10 antibody was a generous gift from Tim Hunt. Cdh1, pT14Cdk1, and Nucleolin antibodies were from Abcam (Cambridge, MA); cyclin B1 antibody was from BD Biosciences (San Jose, CA); Cdc20(p55) antibody was a gift from Jasmin Weinstein (Amgen, Thousand Oaks, CA), securin-1 antibody was from Zymed; pY15Cdk1, pS10 histone H3, Wee1, anti-Myt1Cdc25C, and Cdk1 antibodies were from Cell Signaling. MastL antibody was from Abcam. Primary antibodies were detected using horseradish-peroxidase conjugated immunoglobulin G (IgG) (Jackson ImmunoResearch, West Grove, PA) and visualized using the West Pico Chemiluminescent kit (Pierce, Rockford, IL). For pNucleolin and β -actin Western blots associated with Cdk1/cyclin B1 kinase assays in Figure 6C, secondary antibodies used were labeled with Alexa-488 and Alexa-568 (Invitrogen), and these membranes were scanned with a Typhoon 9400 PhosphorImager (Amersham, Piscataway, NJ).

Flow cytometry

For pS10 histone H3 analysis, cells were treated as detailed in figure legends, trypsinized and fixed in 2% formaldehyde in PHEM (60 mM PIPES, 25 mM HEPES [pH 6.8], 10 mM EDTA, 4 mM MgCl₂) for 15 min, then permeabilized with 90% methanol at –20°C. Later, cells were washed three times with phosphate-buffered saline (PBS), blocked with 5% BSA in PBS and labeled with anti-pS10 Histone H3 antibody conjugated to Alexa Fluor 647 (Cell Signaling). Analysis was carried out on a FACSCalibur flow cytometer (BD Biosciences).

Live imaging

Cells were grown either on 25-mm glass coverslips, which were inserted in an Attofluor culture chamber (Molecular Probes, Eugene,

OR) before the experiment, or in Lab-Tek Chambered Coverglass multiwell dishes. *Xenopus* S3 cells were imaged at room temperature in their normal growth medium. HeLa cells were imaged in L-15 medium with 10% FBS at 37°C. Temperature was maintained with an air curtain incubator (Nevtek, Burnsville, VA) and an objective heater (Biopetech, Butler, PA). Time-lapse phase contrast and fluorescence images were collected using a Zeiss Axiovert 200M wide-field fluorescence microscope. The microscope was equipped with Hamamatsu ORCA-ERG digital camera. A 40 \times Plan-Neofluar oil immersion objective was used for most live imaging experiments. Drugs were substituted by addition of concentrated stock solutions to the live imaging media or by exchange of the media. Images were processed using the Metamorph software (Molecular Devices, Sunnyvale, CA).

Immunofluorescence

HeLa cells were grown on glass coverslips and treated as detailed in the figure legends. Cells were fixed in 2% paraformaldehyde/PHEM solution containing 0.5% Triton X-100 for 15 min. Coverslips were washed in PBST, blocked in 5%BSA/PBS, and incubated overnight with primary antibodies. Samples were then incubated with secondary antibodies for 2–3 h, stained with DNA dye, DAPI, and mounted using Vectashield (Vector Laboratories, Burlingame, CA). For data displayed in Figure 3 and Supplemental Figures 2 and 5, the following antibodies were used: mouse MPM2 (Dako Corp, Oregon City, OR), rabbit pS-Cdk (Cell Signaling) or mouse IgM pNucleolin (a gift from P. Davies). Each sample was coincubated with an antibody against the Lamin B1, either of mouse or of rabbit origin (both from Abcam). Secondary goat anti-rabbit and goat anti-mouse or anti-mouse IgM antibodies were conjugated to Cy3 and FITC (Jackson ImmunoResearch). DNA was stained with DAPI. The images were acquired using Zeiss Axiovert 200M wide-field fluorescence microscope (40 \times oil immersion objective) equipped with a Hamamatsu ORCA-ERG digital camera and processed with MetaMorph (Molecular Devices).

For data displayed in Figure 4, cells were labeled with rat antibody against tyrosinated alpha-tubulin (clone YL1/2; Abcam) followed by a secondary goat anti-rat antibody conjugated to Cy3. Subsequently, cells were labeled with mouse anti-pS10 Histone H3 antibody conjugated to Alexa Fluor 647 (Cell Signaling). DNA was stained with Vybrant DyeCycle Green (Molecular Probes). For data displayed in Supplemental Figure 3, cells were first labeled with primary mouse antibody against nucleolin (Abcam) and secondary goat anti-mouse antibody conjugated to Cy5. Subsequently, cells were labeled with phospho-Nucleolin mouse IgM antibody and the secondary antibody against mouse IgM conjugated to Cy3. DNA was stained with Vybrant DyeCycle Green. Images from these experiments were collected using a 63 \times PlanApochromat oil immersion objective on a Zeiss AxioObserver equipped with a high-speed Yokogawa CSU 22 spinning disk confocal imaging system and a Hamamatsu ORCA-ERG digital camera. Images were collected and processed with SlideBook software (Intelligent Imaging Innovations, Denver, CO).

Quantitative image analysis

To measure the fluorescent cyclin B1-GFP degradation in living cells, time-lapse images were collected at 1-min intervals. The region was drawn around each cell to be measured, and the identical region was placed in an area without fluorescent objects to be used for background subtraction. The net average fluorescence intensity of a pixel in the region of interest was calculated for each time point. Because cells expressed different levels of fluorescent

cyclin B, the net average intensity values were normalized to the initial (first time point) value that was designated as 1. Averages of normalized intensity values of at least five identically treated cells were calculated for each time point and plotted on a graph. For these experiments, all parameters during image acquisition were the same.

To measure fluorescence intensities of MPM2, pS-Cdk, and pNucleolin antibody labeling, 1- μ m Z-stacks through cells of different stages of mitosis were acquired. A region was drawn around each cell to be measured, and the same size region was drawn in an area without fluorescent objects to be used for background subtraction. The net integrated intensity for each cell was measured at a single Z plane with highest integrated intensity values in the region of interest (this was usually the plane with the best focus). The weak signal from interphase cells was designated as 1, and the fluorescence intensity values at each mitotic stage were normalized and plotted relative to interphase. Each bar represents an average of 15–30 cells. The intensity of a signal from the control slide labeled with secondary antibodies alone was comparable to the intensity of the background in experimental samples.

Cdk1/Cyclin B1 kinase assays

HeLa cells were grown in 60-mm plates, synchronized by double thymidine block, and then treated as detailed in figure legend. Each plate represented an experimental sample. Samples were collected by trypsinization and lysed in RIPA (150 mM NaCl, 0.5% sodium deoxycholate, 0.1% SDS, and 50 mM TrisHCl, pH 7.4, 1%NP-40) supplemented with 10 mM EGTA and HALT Protease and Phosphatase inhibitor cocktail (Pierce). A portion of lysate was saved for the Western blotting analysis. Cdk1/cyclin B1 complex was immunoprecipitated with cyclin B1 monoclonal antibody (mAb) (BD Biosciences) on protein A/G agarose resin (Pierce). For kinase reaction, immunoprecipitates were incubated in kinase buffer (25 mM Tris-HCl [pH 7.5], 5 mM beta-glycerophosphate, 2 mM DTT, 0.1 mM Na₃VO₄, 10 mM MgCl₂). Each reaction contained 1–2 mg/ml Histone H1, 200 μ M ATP, and 1 μ Ci of [³²P]ATP. Reactions were incubated at 37°C for 20 min, stopped by addition of SDS sample buffer, and separated by SDS-PAGE in 4–12% Bis-Tris gels (Invitrogen). The gel was exposed to a phosphor screen (Amersham), which was then scanned with a Typhoon 9400 PhosphorImager (Amersham). The gel was subsequently stained with Coomassie Blue.

ACKNOWLEDGMENTS

We express our tremendous appreciation to Bela Novak for critical reading of the manuscript and for his astute comments and suggestions. We are grateful to Jonathon Pines, Randall King, Peter Davies, and Osamu Hashimoto for generously providing essential reagents. We thank Pfizer for providing PD0166285. We are grateful to Todd Stukenberg, Jonathon Pines, Andrew Murray, Peter Lenart, Mark Terasaki, and Boris Rubinstein for insightful discussions. We thank the OMRF flow cytometry core facility for technical assistance. We thank the members of the Gorbsky, Dresser, and Li laboratories for help and advice. Special thanks go to Sreekumar Ramachandran for help with kinase assays. The work in G.J.G.'s laboratory was supported by Grant 2R01GM050412 from the National Institute of General Medical Sciences and by the McCasland Foundation.

REFERENCES

Amon A (2008). A decade of Cdc14—a personal perspective. Delivered on 9 July 2007 at the 32nd FEBS Congress in Vienna, Austria. FEBS J 275, 5774–5784.

Andreeva AV, Kutuzov MA (2001). PPP family of protein Ser/Thr phosphatases: two distinct branches? Mol Biol Evol 18, 448–452.

Androic I, Kramer A, Yan R, Rodel F, Gatje R, Kaufmann M, Strebhardt K, Yuan J (2008). Targeting cyclin B1 inhibits proliferation and sensitizes breast cancer cells to taxol. BMC Cancer 8, 391.

Arooz T, Yam CH, Siu WY, Lau A, Li KK, Poon RY (2000). On the concentrations of cyclins and cyclin-dependent kinases in extracts of cultured human cells. Biochemistry 39, 9494–9501.

Bellanger S, de Gramont A, Sobczak-Thépot J (2007). Cyclin B2 suppresses mitotic failure and DNA rereplication in human somatic cells knocked down for both cyclins B1 and B2. Oncogene 26, 7175–7184.

Bentley AM, Normand G, Hoyt J, King RW (2007). Distinct sequence elements of cyclin B1 promote localization to chromatin, centrosomes, and kinetochores during mitosis. Mol Biol Cell 18, 4847–4858.

Berdougo E, Nachury MV, Jackson PK, Jallepalli PV (2008). The nucleolar phosphatase Cdc14B is dispensable for chromosome segregation and mitotic exit in human cells. Cell Cycle 7, 1184–1190.

Bialojan C, Takai A (1988). Inhibitory effect of a marine-sponge toxin, okadaic acid, on protein phosphatases. Specificity and kinetics. Biochem J 256, 283–290.

Boisvert FM, van Koningsbruggen S, Navascues J, Lamond AI (2007). The multifunctional nucleolus. Nat Rev Mol Cell Biol 8, 574–585.

Bollen M, Gerlich DW, Lesage B (2009). Mitotic phosphatases: from entry guards to exit guides. Trends Cell Biol 19, 531–541.

Booher RN, Holman PS, Fattaey A (1997). Human Myt1 is a cell cycle-regulated kinase that inhibits Cdc2 but not Cdk2 activity. J Biol Chem 272, 22300–22306.

Bosl WJ, Li R (2005). Mitotic-exit control as an evolved complex system. Cell 121, 325–333.

Burgess A, Vigneron S, Brioudes E, Labbe JC, Lorca T, Castro A (2010). Loss of human Greatwall results in G2 arrest and multiple mitotic defects due to deregulation of the cyclin B-Cdc2/PP2A balance. Proc Natl Acad Sci USA 107, 12564–12569.

Castilho PV, Williams BC, Mochida S, Zhao Y, Goldberg ML (2009). The M phase kinase Greatwall (Gwl) promotes inactivation of PP2A/B55delta, a phosphatase directed against CDK phosphosites. Mol Biol Cell 20, 4777–4789.

Chen Q, Zhang X, Jiang Q, Clarke PR, Zhang C (2008). Cyclin B1 is localized to unattached kinetochores and contributes to efficient microtubule attachment and proper chromosome alignment during mitosis. Cell Res 18, 268–280.

Clute P, Pines J (1999). Temporal and spatial control of cyclin B1 destruction in metaphase. Nat Cell Biol 1, 82–87.

Cogswell JP, Godlevski MM, Bonham M, Bisi J, Babiss L (1995). Upstream stimulatory factor regulates expression of the cell cycle-dependent cyclin B1 gene promoter. Mol Cell Biol 15, 2782–2790.

Davis FM, Tsao TY, Fowler SK, Rao PN (1983). Monoclonal antibodies to mitotic cells. Proc Natl Acad Sci USA 80, 2926–2930.

De Wulf P, Montani F, Visintin R (2009). Protein phosphatases take the mitotic stage. Curr Opin Cell Biol 21, 806–815.

den Elzen N, Pines J (2001). Cyclin A is destroyed in prometaphase and can delay chromosome alignment and anaphase. J Cell Biol 153, 121–136.

Dephoure N, Zhou C, Villen J, Beausoleil SA, Bakalarski CE, Elledge SJ, Gygi SP (2008). A quantitative atlas of mitotic phosphorylation. Proc Natl Acad Sci USA 105, 10762–10767.

Dohadwala M, da Cruz e Silva EF, Hall FL, Williams RT, Carbonaro-Hall DA, Nairn AC, Greengard P, Berndt N (1994). Phosphorylation and inactivation of protein phosphatase 1 by cyclin-dependent kinases. Proc Natl Acad Sci USA 91, 6408–6412.

Dranovsky A, Vincent I, Gregori L, Schwarzman A, Colflesh D, Enghild J, Strittmatter W, Davies P, Goldgaber D (2001). Cdc2 phosphorylation of nucleolin demarcates mitotic stages and Alzheimer's disease pathology. Neurobiol Aging 22, 517–528.

Gavet O, Pines J (2010a). Activation of cyclin B1-Cdk1 synchronizes events in the nucleus and the cytoplasm at mitosis. J Cell Biol 189, 247–259.

Gavet O, Pines J (2010b). Progressive activation of CyclinB1-Cdk1 coordinates entry to mitosis. Dev Cell 18, 533–543.

Geley S, Kramer E, Gieffers C, Gannon J, Peters JM, Hunt T (2001). Anaphase-promoting complex/cyclosome-dependent proteolysis of human cyclin A starts at the beginning of mitosis and is not subject to the spindle assembly checkpoint. J Cell Biol 153, 137–148.

Glutzer M, Murray AW, Kirschner MW (1991). Cyclin is degraded by the ubiquitin pathway. Nature 351, 132–138.

Gong D, Pomerening JR, Myers JW, Gustavsson C, Jones JT, Hahn AT, Meyer T, Ferrell JE Jr (2007). Cyclin A2 regulates nuclear-envelope breakdown and the nuclear accumulation of cyclin B1. Curr Biol 17, 85–91.

- Hagting A, Jackman M, Simpson K, Pines J (1999). Translocation of cyclin B1 to the nucleus at prophase requires a phosphorylation-dependent nuclear import signal. *Curr Biol* 9, 680–689.
- Hagting A, Karlsson C, Clute P, Jackman M, Pines J (1998). MPF localization is controlled by nuclear export. *EMBO J* 17, 4127–4138.
- Hashimoto O, Shinkawa M, Torimura T, Nakamura T, Selvendiran K, Sakamoto M, Koga H, Ueno T, Sata M (2006). Cell cycle regulation by the Wee1 inhibitor PD0166285, pyrido [2,3-d] pyrimidine, in the B16 mouse melanoma cell line. *BMC Cancer* 6, 292.
- Hershko A, Ganoth D, Sudakin V, Dahan A, Cohen LH, Luca FC, Ruderman JV, Eytan E (1994). Components of a system that ligates cyclin to ubiquitin and their regulation by the protein kinase cdc2. *J Biol Chem* 269, 4940–4946.
- Herzog F, Mechtler K, Peters JM (2005). Identification of cell cycle-dependent phosphorylation sites on the anaphase-promoting complex/cyclosome by mass spectrometry. *Methods Enzymol* 398, 231–245.
- Hoffmann I, Draetta G, Karsenti E (1994). Activation of the phosphatase activity of human cdc25A by a cdk2-cyclin E dependent phosphorylation at the G1/S transition. *EMBO J* 13, 4302–4310.
- Hwang A, Maity A, McKenna WG, Muschel RJ (1995). Cell cycle-dependent regulation of the cyclin B1 promoter. *J Biol Chem* 270, 28419–28424.
- Izumi T, Maller JL (1993). Elimination of cdc2 phosphorylation sites in the cdc25 phosphatase blocks initiation of M-phase. *Mol Biol Cell* 4, 1337–1350.
- Jaspersen SL, Charles JF, Morgan DO (1999). Inhibitory phosphorylation of the APC regulator Hct1 is controlled by the kinase Cdc28 and the phosphatase Cdc14. *Curr Biol* 9, 227–236.
- Jin P, Gu Y, Morgan DO (1996). Role of inhibitory CDC2 phosphorylation in radiation-induced G2 arrest in human cells. *J Cell Biol* 134, 963–970.
- Kallio M, Weinstein J, Daum JR, Burke DJ, Gorbsky GJ (1998). Mammalian p55CDC mediates association of the spindle checkpoint protein Mad2 with the cyclosome/anaphase-promoting complex, and is involved in regulating anaphase onset and late mitotic events. *J Cell Biol* 141, 1393–1406.
- Kapuy O, He E, Uhlmann F, Novak B (2009). Mitotic exit in mammalian cells. *Mol Syst Biol* 5, 324.
- Kim SY, Song EJ, Lee KJ, Ferrell JE Jr (2005). Multisite M-phase phosphorylation of Xenopus Wee1A. *Mol Cell Biol* 25, 10580–10590.
- King RW, Deshaies RJ, Peters JM, Kirschner MW (1996). How proteolysis drives the cell cycle. *Science* 274, 1652–1659.
- Kraft C, Herzog F, Gieffers C, Mechtler K, Hagting A, Pines J, Peters JM (2003). Mitotic regulation of the human anaphase-promoting complex by phosphorylation. *EMBO J* 22, 6598–6609.
- Kramer ER, Scheuringer N, Podtelejnikov AV, Mann M, Peters JM (2000). Mitotic regulation of the APC activator proteins CDC20 and CDH1. *Mol Biol Cell* 11, 1555–1569.
- Kwon YG, Lee SY, Choi Y, Greengard P, Nairn AC (1997). Cell cycle-dependent phosphorylation of mammalian protein phosphatase 1 by cdc2 kinase. *Proc Natl Acad Sci USA* 94, 2168–2173.
- Lahav-Baratz S, Sudakin V, Ruderman JV, Hershko A (1995). Reversible phosphorylation controls the activity of cyclosome-associated cyclin-ubiquitin ligase. *Proc Natl Acad Sci USA* 92, 9303–9307.
- Li J, Wang Y, Sun Y, Lawrence TS (2002). Wild-type TP53 inhibits G(2)-phase checkpoint abrogation and radiosensitization induced by PD0166285, a WEE1 kinase inhibitor. *Radiat Res* 157, 322–330.
- Li M, Satinover DL, Brautigan DL (2007). Phosphorylation and functions of inhibitor-2 family of proteins. *Biochem* 46, 2380–2389.
- Lindqvist A, van Zon W, Karlsson Rosenthal C, Wolthuis RM (2007). Cyclin B1-Cdk1 activation continues after centrosome separation to control mitotic progression. *PLoS Biol* 5, e123.
- Matsusaka T, Pines J (2004). Chfr acts with the p38 stress kinases to block entry to mitosis in mammalian cells. *J Cell Biol* 166, 507–516.
- McGowan CH, Russell P (1995). Cell cycle regulation of human WEE1. *EMBO J* 14, 2166–2175.
- Mikhailov A, Shinohara M, Rieder CL (2005). The p38-mediated stress-activated checkpoint. A rapid response system for delaying progression through antepause and entry into mitosis. *Cell Cycle* 4, 57–62.
- Mochida S, Hunt T (2007). Calcineurin is required to release Xenopus egg extracts from meiotic M phase. *Nature* 449, 336–340.
- Mochida S, Ieko S, Gannon J, Hunt T (2009). Regulated activity of PP2A-B55 delta is crucial for controlling entry into and exit from mitosis in Xenopus egg extracts. *EMBO J* 28, 2777–2785.
- Musacchio A, Salmon ED (2007). The spindle-assembly checkpoint in space and time. *Nat Rev Mol Cell Biol* 8, 379–393.
- Nousiainen M, Sillje HH, Sauer G, Nigg EA, Korner R (2006). Phosphoproteome analysis of the human mitotic spindle. *Proc Natl Acad Sci USA* 103, 5391–5396.
- Novak B, Tyson JJ (1993). Numerical analysis of a comprehensive model of M-phase control in Xenopus oocyte extracts and intact embryos. *J Cell Sci* 106, Pt 41153–1168.
- Peters JM, King RW, Hoog C, Kirschner MW (1996). Identification of BIME as a subunit of the anaphase-promoting complex. *Science* 274, 1199–1201.
- Piaggio G, Farina A, Perrotti D, Manni I, Fuschi P, Sacchi A, Gaetano C (1995). Structure and growth-dependent regulation of the human cyclin B1 promoter. *Exp Cell Res* 216, 396–402.
- Pines J, Hunter T (1991). Human cyclins A and B1 are differentially located in the cell and undergo cell cycle-dependent nuclear transport. *J Cell Biol* 115, 1–17.
- Pomerening JR, Kim SY, Ferrell JE Jr (2005). Systems-level dissection of the cell-cycle oscillator: bypassing positive feedback produces damped oscillations. *Cell* 122, 565–578.
- Pomerening JR, Sontag ED, Ferrell JE Jr (2003). Building a cell cycle oscillator: hysteresis and bistability in the activation of Cdc2. *Nat Cell Biol* 5, 346–351.
- Pomerening JR, Ubersax JA, Ferrell JE Jr (2008). Rapid cycling and precocious termination of G1 phase in cells expressing CDK1A^F. *Mol Biol Cell* 19, 3426–3441.
- Potapova TA, Daum JR, Byrd KS, Gorbsky GJ (2009). Fine tuning the cell cycle: activation of the Cdk1 inhibitory phosphorylation pathway during mitotic exit. *Mol Biol Cell* 20, 1737–1748.
- Potapova TA, Daum JR, Pittman BD, Hudson JR, Jones TN, Satinover DL, Stukenberg PT, Gorbsky GJ (2006). The reversibility of mitotic exit in vertebrate cells. *Nature* 440, 954–958.
- Pu L, Amoscatto AA, Bier ME, Lazo JS (2002). Dual G1 and G2 phase inhibition by a novel, selective Cdc25 inhibitor 6-chloro-7-[corrected] (2-morpholin-4-ylethylamino)-quinoline-5,8-dione. *J Biol Chem* 277, 46877–46885.
- Rudner AD, Murray AW (2000). Phosphorylation by Cdc28 activates the Cdc20-dependent activity of the anaphase-promoting complex. *J Cell Biol* 149, 1377–1390.
- Sha W, Moore J, Chen K, Lassaletta AD, Yi CS, Tyson JJ, Sible JC (2003). Hysteresis drives cell-cycle transitions in Xenopus laevis egg extracts. *Proc Natl Acad Sci USA* 100, 975–980.
- Shteinberg M, Protopopov Y, Listovsky T, Brandeis M, Hershko A (1999). Phosphorylation of the cyclosome is required for its stimulation by Fizzy/cdc20. *Biochem Biophys Res Commun* 260, 193–198.
- Steen JA, Steen H, Georgi A, Parker K, Springer M, Kirchner M, Hamprecht F, Kirschner MW (2008). Different phosphorylation states of the anaphase promoting complex in response to antimetabolic drugs: a quantitative proteomic analysis. *Proc Natl Acad Sci USA* 105, 6069–6074.
- Stegmeier F, Amon A (2004). Closing mitosis: the functions of the Cdc14 phosphatase and its regulation. *Annu Rev Genet* 38, 203–232.
- Sudakin V, Ganoth D, Dahan A, Heller H, Hershko J, Luca FC, Ruderman JV, Hershko A (1995). The cyclosome, a large complex containing cyclin-selective ubiquitin ligase activity, targets cyclins for destruction at the end of mitosis. *Mol Biol Cell* 6, 185–197.
- Sullivan M, Morgan DO (2007). Finishing mitosis, one step at a time. *Nat Rev Mol Cell Biol* 8, 894–903.
- Trinkle-Mulcahy L, Lamond AI (2006). Mitotic phosphatases: no longer silent partners. *Curr Opin Cell Biol* 18, 623–631.
- Tyson JJ, Novak B (2001). Regulation of the eukaryotic cell cycle: molecular antagonism, hysteresis, and irreversible transitions. *J Theor Biol* 210, 249–263.
- Ubersax JA, Woodbury EL, Quang PN, Paraz M, Blethrow JD, Shah K, Shokat KM, Morgan DO (2003). Targets of the cyclin-dependent kinase Cdk1. *Nature* 425, 859–864.
- Vazquez-Novelle MD, Esteban V, Bueno A, Sacristan MP (2005). Functional homology among human and fission yeast Cdc14 phosphatases. *J Biol Chem* 280, 29144–29150.
- Vigneron S, Brioudes E, Burgess A, Labbe JC, Lorca T, Castro A (2009). Greatwall maintains mitosis through regulation of PP2A. *EMBO J* 28, 2786–2793.
- Virshup DM, Shenolikar S (2009). From promiscuity to precision: protein phosphatases get a makeover. *Mol Cell* 33, 537–545.
- Visintin R, Craig K, Hwang ES, Prinz S, Tyers M, Amon A (1998). The phosphatase Cdc14 triggers mitotic exit by reversal of Cdk-dependent phosphorylation. *Mol Cell* 2, 709–718.
- Vodermaier HC, Peters JM (2004). APC activators caught by their tails? *Cell Cycle* 3, 265–266.

- Voets E, Wolthuis RM (2010). MASTL is the human orthologue of Greatwall kinase that facilitates mitotic entry, anaphase and cytokinesis. *Cell Cycle* 9, 3591–3601.
- Wang Y, Li J, Booher RN, Kraker A, Lawrence T, Leopold WR, Sun Y (2001). Radiosensitization of p53 mutant cells by PD0166285, a novel G(2) checkpoint abrogator. *Cancer Res* 61, 8211–8217.
- Watanabe N, Broome M, Hunter T (1995). Regulation of the human WEE1Hu CDK tyrosine 15-kinase during the cell cycle. *EMBO J* 14, 1878–1891.
- Wei Y, Yu L, Bowen J, Gorovsky MA, Allis CD (1999). Phosphorylation of histone H3 is required for proper chromosome condensation and segregation. *Cell* 97, 99–109.
- Wu JQ, Guo JY, Tang W, Yang CS, Freel CD, Chen C, Nairn AC, Kornbluth S (2009). PP1-mediated dephosphorylation of phosphoproteins at mitotic exit is controlled by inhibitor-1 and PP1 phosphorylation. *Nat Cell Biol* 11, 644–651.
- Yuan J, Kramer A, Matthes Y, Yan R, Spankuch B, Gatje R, Knecht R, Kaufmann M, Strebhardt K (2006). Stable gene silencing of cyclin B1 in tumor cells increases susceptibility to taxol and leads to growth arrest in vivo. *Oncogene* 25, 1753–1762.
- Yuan J, Yan R, Kramer A, Eckerdt F, Roller M, Kaufmann M, Strebhardt K (2004). Cyclin B1 depletion inhibits proliferation and induces apoptosis in human tumor cells. *Oncogene* 23, 5843–5852.